UNIVERSITY OF CALIFORNIA, SAN DIEGO

Interaction Between NF-κB RelB and Apoptotic Modulator Daxx

A thesis submitted in partial satisfaction of the requirements
for the degree of Master of Science

in

Chemistry

by

Jee-Sun Kim

Committee in charge:

Professor Gourisankar Ghosh, Chair
Professor John Czworkowski
Professor Hector Viadiu-Ilarraza

2013

The Thesis of Jee-Sun Kim is approved and it is acceptable in quality and form for publication on microfilm and electronically:

Chair

University of California, San Diego

2013

DEDICATION

I would like to dedicate this thesis to God through whom all things are possible (Philippians 4:13).

TABLE OF CONTENTS

LIST OF ABBREVIATIONS

ARD	Ankyrin repeat domain
βME	2-Mercaptoethanol
CV	Column volume
Daxx	Death domain associated protein
DD	Dimerization Domain
DISC	Death-induced signaling complex
DHB	Daxx helix bundle
DNMT	DNA methyltransferase
DTT	Dithiothreitol
EDTA	Ethylenediaminetetraacetic acid
GST	Glutathione S-Transferase
HRP	Horseradish peroxidase
IκB	Inhibitor of NF-κB
IKK	IκB kinase complex
IL-1	Interleukin 1
IPTG	Isopropylthio-β-D-galactoside
JNK	c-Jun *N*-terminal Kinase
kDa	Kilodalton
LB	Lysogeny Broth
LPS	Lipopolysaccharides
LTβ	Lymphotoxin β

MES	2-Morpholinoethanesulfonic acid
MOMP	Mitochondrial outer-membrane permeabilization
MWCO	Molecular weight cutoff
NEMO	NF-κB Essential Modulator
NF-κB	Nuclear factor of kappa gene transcription in B cells
O.D.	Optical density
PAGE	Polyacrylamide gel electrophoresis
PAH	Paired amphipathic helices
PCR	Polymerase chain reaction
PMSF	Phenylmethylsulfonylfluoride
RHR	Rel homology region
RPM	Rotations per minute
ΣPIC	Sigma protease inhibitor cocktail
SDS	Sodium dodecyl sulfate
SUMO	Small ubiquitin-like modifier protein
TAD	Trans Activation Domain
TEV	Tobacco etch virus
TNF-α	Tumor necrosis factor α
Tris	Tris(hydroxymethyl)aminomethane
UV	Ultraviolet
V	Volts

LIST OF FIGURES

LIST OF TABLES

ACKNOWLEDGEMENTS

I would like to thank my advisor, Dr. Gourisankar Ghosh, who has continually supported, motivated, and encouraged me to be the best scientist that I can be. Without his help, I could not have made it this far. I am very grateful for his patience, challenges, humor, and life advice. He has been a great mentor who has left a great impact and legacy in my life.

I would also like to thank my thesis committee advisor, Dr. John Czworkowski who has been a wonderful teacher and a friend. He was my professor for General Chemistry class during freshman year, and through his passion for teaching and love for science, I have also come to love science.

I would like to thank my other thesis committee advisor, Dr. Hector Viadiu whose gentleness and support have been great sources of encouragement and motivation. He helped me appreciate Biochemistry, as well as scientific research, and I am very thankful for his genuine help and support.

I would like to thank the following past and present members of the Ghosh Lab for their tremendous guidance and assistance: Dr. Amanda Fusco-Hernandez, Dr. Kaushik Saha, Dr. Yidan Li, Dr. Smarajit Polley, Dr. Sulakshana Mukherjee, Dr. Zhihua Tao, Dr. Suhyung Cho, Dr. Vivien Wang, Dr. Mari Mulero-Roig, Dr. Abantika Ganguli, Dr. Tapan Biswas, Dr. Xiang-Yang Zhong, Dr. De-Bin Huang, Kevin Carman, Stephan Leung, Monique Peña, Annapurna Vemu, Amy Hoang, Patrick Tien, and Ruina Li.

Finally, I would like to thank my family and friends who have supported me immensely.

ABSTRACT OF THE THESIS

Interaction Between NF-κB RelB and Apoptotic Modulator Daxx

by

Jee-Sun Kim

Master of Science in Chemistry

University of California, San Diego, 2013

Professor Gourisankar Ghosh, Chair

Two proteins important in transcriptional regulation and apoptotic modulation are RelB and Daxx. Previously, it was shown that Daxx induced apoptosis through interaction with RelB to silence Daxx transcriptional activity. The main focus of this study was to identify the binding domains required for such interaction and to purify the recombinant RelB:Daxx heterodimer from *E.coli* for x-ray crystallography analysis. The findings showed that Daxx DHBI (56-144) region interacts with RelB DD (277-391). This finding was confirmed through GST pulldown analysis with different fragments of Daxx and RelB. Some of the RelB DD mutants (I335F; I286M, I335F; and Y300F, I335F) which can enhance the binding ability of RelB DD were shown to abrupt the interaction with Daxx DHBI. Surprisingly, it was found that the strength of interaction with RelB RHR (1-400) and Daxx DHBI was not strong enough to be able to be purified as a single

peak complex via gel filtration. While Daxx and RelB are known to interact with each other to induce apoptosis, the binding affinity is not strong enough perhaps due to competition with other NF-κB factors binding to the open interface of RelB DD. In order to get a more stable Daxx:RelB complex, future studies can focus on the expression and purification of Daxx *N*-terminus (1-400) and RelB RHR (1-400) complex. Also, purification and crystallization of RelB DD mutants can give better understanding about the dimerization domain behavior and as well as their effect in binding to Daxx.

I. Introduction

A. NF-κB Transcription Factors

NF-κB transcription factors are B cell nuclear factors that have important functions in biology. They are involved in immune system, cell survival pathway, and inflammatory pathways (Sun et al., 2011). Twenty seven years ago, they were first discovered as nuclear proteins that specifically interact with the κ immunoglobulin enhancer to help immunoglobulin light chain genes be transcribed (Sen et al., 1986).

Upon external stimuli such as TFN, IL-1, LPS, or T cell activators, the NF-κB pathway is activated. Other stimuli can also induce this pathway including UV exposure, viral infection, and growth factors. In resting cells, NF-κB is bound by IκB, which is an inhibitory protein of NF-κB. Upon exposure to the relevant inducer, NF-κB can be activated to regulate the transcription of certain genes within minutes (Baldwin, 1996). The cellular stimuli activate IKK (kappa B kinase) which in turn phosphorylates IκB as a signal for proteosomal degradation, which then releases NF-κB dimers inside the nucleus, thereby activating gene regulation and transcription.

There are five main genes in NF-κB family (**Figure 1)**: RelA (p65), RelB, c-Rel, p52 (processed from precursor protein p100), and p50 (processed from precursor protein p105). These five proteins share a Rel Homology Domain (RHD), which are the first 300 amino acids from the *N*-terminal side that are important in forming body pattern and immune system in insect models (Baldwin, 1996).

There are two main pathways in NF-κB signaling: the canonical and non-canonical pathways (**Figure 2**). In the canonical pathway, upon degradation of IκB, NF-

κB complex is released and translocated into the nucleus as dimmers. p50:RelA dimer is the most abundant dimer in this pathway(Hayden et al., 2008; Vallabhapurapu et al., 2009). The main IKK trimeric complex responsible for phosphorylation of IκB is composed of IKKα and IKKβ, which are the catalytic subunits, and IKKγ, which is a regulatory unit also known as NF-κB essential modulator (NEMO) (Sun et al., 2008). p100 is inducibly processed into p52, which forms a complex with RelB in the non-canonical pathway (Sun et al., 2011).

Unlike other transcription factor binding domains, NF-κB has a very large DNA binding domain which makes contact with the RHD of NF-κB. Structural studies revealed that similar to the immunoglobulin factors, the RHD has two domains that are folded into. There is a high similarity of this overall structure of the RHD in NF-κB family with the DNA binding in each NF-κB member (Baldwin, 1996). The presence of dimerization domains allows the formation of homodimers or heterodimers of different NF-κB members (**Figure 3**).

B. Dimerization Domain of RelB

In particular, the *rel* oncogene shares strong homology with p60 and p65, as shown in **Figure 4** (Ruben et al., 1992). RelB was first discovered in fibroblasts stimulated by serum. It has an important function in developing lymphoid organs (Moorthy *et al.*, 2007). RelB has a tendency to form a heterodimer with p50 or p52 and bind to various κB sites as evidenced from the electrophoretic mobility shift assay result. RelB:p50 heterodimer is important as it serves as a strong transcription transactivator in vivo. By forming such heterodimer, RelB carries various roles in gene transcriptional

regulation (Ryseck et al., 1992). Since the discovery that RelB forms a heterodimer with p50, understanding the structural mechanism of RelB dimerization by elucidating its dimerization domain function has been an ongoing interest. In order to fully transactivate genes, both N- and C- termini of RelB are important (**Figure 5; Figure 6**). The extended *N*-terminus of RelB forms a leucine zipper-like motif which is crucial in activating transcription (Dobrzanski et al., 1993). The most important residue that is essential in RelB dimer formation is Y300. The dimerization domain surface of RelB is largely nonpolar which promotes the formation of hydrogen bonds. Through the intertwining mechanism, hydrogen bonds become more stabilized as an extra β sheet is created at the dimerization domain interface (**Figure 7**). The transiently stable RelB can be prevented from degradation, allowing it to dimerize with other NF-κB factors (Hung *et al.*, 2005). It was also discovered that when there is a mutation in the dimerization domain of RelB, its structure completely changes because the mutation affects the dimerization domain ability of RelB dimers. In particular, mutations in two amino acid residues have a significant effect in changing RelB dimer formation. This implies that these two amino acid residues are important in RelB dimerization domain as their mutations have the ability to change the conformation. The presence of specific amino acids in RelB dimerization domain allow for selective dimerization with other NF-κB factors such as p50 and p52 (Vu *et al.*, 2013).

C. Daxx Interaction with RelB

It was previously found that Daxx interacts with various anti-apoptotic genes regulated by NF-κB to repress their expression (**Figure 8**). Since NF-κB transcription

factors are related to cell survival, Daxx represses their expression by inhibiting human cIAP2 gene promoter transcriptional activation moderated by RelB. Electrophoretic mobility shift assays show that while RelB is bound to cIAP2 promoter target sites, Daxx interacts and binds to RelB. In daxx$^{-/-}$ mouse embryos, the levels of protein and mRNA of *murine* c-IAP are high. In relB$^{-/-}$ cells, however, c-IAP protein and mRNA levels are low. These data suggest that Daxx represses RelB-mediated transcription to sensitize it to apoptosis. This is done by repressing RelB through its association, although it does not prevent RelB from binding to the target sites. By recruiting other transcription-related factors such as DNA methyltransferases and/or histone deacetylases to RelB promoters, Daxx can cause reduction in transcription expression. Since RelB has various roles in cell, the effects of Daxx might be more complex, and it is possible that Daxx might interact with other transcription factor targets that can also result in the same effect in apoptosis sensitization (Croxton *et al.*, 2006).

Another study pointed out a fact that Daxx and RelB have strong binding to each other. Daxx directly interferes with RelB transcription by repressing its target genes such as: *dapk1*, *dapk3*, c-*flip*, and *birc3* (*ciap2*). In daxx$^{-/-}$ cells, methylation of these target promoters is significantly reduced, whereas reconstitution with Daxx causes DNA methylation to come back. DNA methyl transferase 1 (Dnmt1) is one example of methylation factor that is recruited by Daxx. As shown in **Figure 37,** Daxx can effectively convert RelB from transcription activator to repressor by recruiting DNA methyltransferase such as Dnmtases since Daxx itself does not have DNA binding domain while RelB has a Daxx-interacting domain motif (DID) (Puto *et al.*, 2007). This is a good example of epigenetic silencing that can have many implications in epigenetic-

related drugs important in cancer. This also provides an example where Daxx serves its dual functions as a transcription repressor and apoptotic modulator in epigenetic regulation and transcriptional repression.

D. Daxx as an Apoptotic Modulator

Daxx (Death Doman Associated Protein) has been a protein of ongoing research interest because of its diverse interacting abilities with other transcription factors such as ETS1 (Li et al., 2000), p53 (Zhang et al., 2012). It is known as a Fas-binding protein involved in the activation of JNK pathway by modulating the induction of apoptosis (Yang et al., 1997). Death-inducing signaling complex (DISC) has various components that can induce apoptosis aided by the binding of various proteins such as Fas-associated death domain (FADD), TNF-receptor-associated death domain (TRADD), receptor-interacting protein kinase 1 (RIP1) and death-associated protein (Daxx) that can recognize the death domain (DD) of death receptors inside the cell surface (Curtin et al., 2003). In particular, Daxx has high expression throughout the body particularly in the thymus and testes. In normal cell state, Daxx mainly associates with other subnuclear factors inside a nucleus, as well as various proteins in cellular processes. Daxx has several domains that are structurally characterized: two amphipathic helices (PAHs) paired by *N*-terminal regions, a *C*-terminal region characterized by the rich presence of serine/proline/threonine, an acidic region, and a coiled-coil domain, as shown in **Figure 9** and **Figure 10** (Salomoni et al., 2006). Due to its interesting role in biology, several X-ray crystallography data have been found. For example, Daxx and Histone complex structure has been solved which showed that Daxx can specifically recognize H3.3

instead of H3.1 (Liu et al., 2012). In addition, Daxx SIM Phosphorylation was further elucidated due to its structural discovery in SUMO paralog-selective binding (Chang et al., 2011) since previously, the SUMO interacting motifs of Daxx have been structurally analyzed (Escobar-Cabrera et al., 2011). Daxx in a complex with a protein such as Rassf1C was discovered in NMR structure that shows how the helical bundles in Daxx make a cleft around their helices for binding (Escobar-Cabrera et al., 2010).

E. Purpose of the Project

The main goal of this project is to understand the domain organization requirement for the binding between Daxx and RelB. Since it was previously known that Daxx and RelB interact *in vivo*, the focus of this study is to replicate this result *in vitro* and to further identify the regions between Daxx and RelB that are sufficient and required for binding to occur. This study would enrich the previous finding by adding more information about in vitro behavior between Daxx and RelB, and this can potentially turn into a crystallization target if Daxx:RelB complex can be purified stably and clean. As a result of in vitro analysis and X-ray crystallography, the project's focus is to identify which regions of Daxx and RelB are required for binding, and which regions are required for complex purification that can be potentially used for crystallization studies.

II. Material and Methods

A. Preparation of *E.coli* Expression Plasmids

All vectors used for cloning were commercially purchased from Novagen with the exception of some modifications.

1. RelB Expression Plasmids

Table 1 shows a list of primers used for sub-cloning RelB inserts into pET24d TEV vector. pET24d TEV vector is based on PET24d, but instead of thrombin cut-site, TEV protease cut-site was inserted, while keeping the His tag still intact. The murine RelB DD (227-391) gene was amplified by polymerase chain reaction (PCR) where it was then inserted into pET24d TEV vector using BamHI and HindIII as cut-sites. **Table 2** shows list of RelB DD mutant primers used to generate different RelB DD mutants. Site-directed mutagenesis was performed based on QuikChange protocol from Stratagene. RelB DD pET15b was used to generate single mutants and single mutants were used to generate double mutants.

2. Daxx Expression Plasmids

Table 1 shows list of primers used for sub-cloning Daxx inserts into several different vectors such as GST TEV, pET21d TEV, and pET11a. GST TEV vector is based on pET21a vector where the thrombin cut-site was replaced with a TEV cut-site and the GST tag was replaced with His tag. pET21d TEV vector is based on pET21d vector that has a TEV cut-site instead of a thrombin cut-site.

B. Expression and Purification of Recombinant Proteins

1. Human *N*-Terminal GST-Daxx (1-400) pGEX and Murine RelB RHR (1-400) pET24d

Each of the above plasmids was co-transformed into Rosetta *E.coli* cells. 2L of LB cell culture (Kanamycin: 35 μg/mL; Ampicillin: 100 μg/mL) was grown at 37 °C until the $O.D._{600}$ reached 0.35. IPTG was added to 0.15 mM and the cells were grown at 18 °C for overnight with vigorous shaking to induce protein expression. In order to purify the co-expressed protein, the cells were pelleted in a JLA 8.1 rotor at 3,000 xg for 15 minutes at 4°C. The pellet was resuspended in 150 mL of lysis buffer (20 mM tris pH 7.5, 200 mM NaCl, 10% glycerol, 5 mM imidazole, 5 mM βME, 0.5 mM PMSF, 0.01% ΣPIC). The cells were sonicated on ice at 90%, cycle 9 for 1 min with 1 min rest in between for a total number of three times. The cell lysate was centrifuged at 13,000 xg in a Sorvall SS-34 rotor for 50 min at 4°C and the resulting supernatant was filtered through a 0.8μm filter. The clarified lysate was loaded onto a Ni^{++} column (pre-equilibrated with lysis buffer) at 1 mL/min. The column was washed with wash buffer (20 mM Tris pH 7.5, 200 mM NaCl, 10% glycerol, 25 mM Imidazole, 5 mM βME) until no more protein came off the column as measured by Bradford. Elution buffer (20 mM Tris pH 7.5, 200 mM NaCl, 10% glycerol, 250 mM Imidazole, 5 mM βME) was used to elute the protein from the column. 0.5 mM EDTA and 1 mM DTT were added to the fractions containing protein which were then bound to GST beads (pre-equilibrated with 20 mM tris pH 7.5, 200 mM NaCl, 10% glycerol, 0.5 mM EDTA, 1 mM DTT) for 2 hours at 4 °C. The beads were then washed with 200 mL of the same buffer and the protein was eluted with 10 mM glutathione pH 7.5 in the same buffer. All the samples were analyzed on a 10%

SDS-PAGE gel. Proteins were concentrated using Centricon 30kDa MWCO and stored at 0.21 mg/ml concentration at -80 °C.

2. Murine p50 RHR (37-363) pET11a

The above plasmid was transformed in BL21 DE3 *E.coli* cells. 2L of LB cell culture (Ampicillin: 100 μg/mL) was grown in conditions similar to previously described except the cells were induced when $O.D._{600}$ reached 0.2 with 0.1 mM IPTG for overnight at room temperature (25 °C). Cells were treated in similar conditions as previously described except lysis buffer (low salt buffer) contained (20mM tris pH 7.5, 100 mM NaCl, 5% glycerol, 2 mM EDTA, 0.5 mM PMSF, 10 mM βME). After filtering the soluble lysate through a 0.8 μm filter, the lysate was loaded onto a FastFlow Q column in tandem with FastFlow SP column (with a 2:1 Q column:S column resin ratio). Once the lysate passed through, the Q column was disconnected while S column was washed with 200 mL of low salt buffer. A gradient using 100 mL low salt buffer and 100 mL high salt buffer (low salt + 400 mM NaCl) was used to elute the protein and 2 mL fractions were collected using fraction collector. Peak fractions were checked by Bradford which were analyzed on 10% SDS-PAGE gel, pooled, concentrated to 5.18 mg/mL using Centricon MWCO 30kDa, and stored at -80 °C.

3. Murine p50 DD (245-350) pET29b RBS

The procedures for p50 DD expression and purification were similar to the expression and purification of p50 RHR. Peak fractions were analyzed on 15% SDS-

PAGE gel, pooled, concentrated to 26.7 mg/mL using Centricon 10kDa MWCO and stored at -80 °C.

4. Murine RelB RHR (1-400) pET24d TEV

The plasmid was transformed in BL21 DE3 *E.coli* cells. 2L of LB cell culture (Kanamycin: 35 μg/mL) was grown until $O.D._{600}$ reached 0.3. The culture was induced with 0.1 mM IPTG at room temperature overnight. Protein purification procedure was similar to *Human* Daxx (1-400) pGEX, *Murine* RelB RHR (1-400) pET24D procedures until the Ni^{++} step. Buffers used were lysis buffer (1 M NaCl, 20 mM Tris pH 7.5, 5 mM Imidazole, 5 mM βME), wash buffer (same as lysis buffer except with 25 mM Imidazole), and elution buffer (same as lysis buffer except with 250 mM Imidazole). 1.5 mL fractions were eluted and analyzed through 12.5% SDS-PAGE gel. Fractions were pooled, concentrated to 4.78 mg/mL, and stored at -80 °C.

5. Murine p50 RHR (37-363) pET11a/Murine RelB RHR(1-400) pET24d TEV Heterodimer Formation

Purified p50 RHR and RelB RHR proteins were thawed and mixed in a 1:1.1 ratio of p50 RHR to RelB RHR in 8M urea. The protein was diluted to 0.36 mg/mL in buffer containing 20 mM tris pH 7.5, 250 mM NaCl, 10% glycerol, 0.5 mM EDTA and stirred for 20 min at 25 °C. Then the sample was dialyzed against 2L dialysis buffer (20 mM tris pH 7.5, 250 mM NaCl, 10% glycerol, 5mM βME, 0.5 mM PMSF) at 4 °C with stirring in a 10kDa MWCO dialysis bag. During the first three hours of dialysis, proteins in the dialysis tubing bag were mixed by manually inverting the bag every half an hour to

ensure efficient mixing of the proteins. Afterwards, old dialysis buffer was replaced with 2 L fresh dialysis buffer and manually mixed every half an hour. After the second three hours passed, the old dialysis buffer was replaced by fresh 2L dialysis buffer. After the third three hours passed, old dialysis buffer was replaced with fresh 2L dialysis buffer for overnight dialysis. The next day, the old dialysis buffer was replaced with 2 L fresh dialysis buffer with lower salt concentration (20 mM tris pH7.5, 50 mM NaCl, 10% glycerol, 5 mM βME, 0.5 mM PMSF) for three hours. After three hours, the old buffer was replaced with fresh 2 L low salt dialysis buffer for additional three hours. Then proteins were loaded onto HiTrap S column (pre-equilibrated with low salt buffer) using a peristaltic pump. The column was washed 2 CV low salt buffer. Using the salt gradient from low salt to high salt (low salt buffer + 500 mM NaCl), 1.5 mL fractions were collected and later analyzed on a 12.5% SDS-PAGE gel. The peak protein fractions were pooled, concentrated, to 2.76 mg/mL and stored at -80°C.

6. RelB DD (277-391) pET15b

The above plasmid was transformed into BL21 DE3 *E.coli* cells. 2L of LB cell culture (Ampicillin: 100 μg/mL) was grown until $O.D._{600}$ reached 0.5 and induced with 0.1 mM IPTG for overnight at room temperature with vigorous shaking. Purification procedures were similar to Human Daxx (1-400) pGEX, Murine RelB RHR (1-400) pET24D purification procedures until the Ni^{++} step. The buffers used in purification were lysis buffer (250 mM NaCl, 20 mM Tris pH 7.5, 5mM Imidazole, 10% glycerol, 5mM βME, 0.5 mM PMSF), wash buffer (lysis buffer + 25 mM Imidazole), and elution buffer (lysis Buffer + 250 mM Imidazole). Ten 2 mL fractions were collected and concentrated

to 2 mL to run on the Superset 75 gel filtration column with gel filtration buffer (200 mM NaCl, 2 0mM tris pH 7.5, 10% glycerol, 1 mM DTT). Peak fractions from the SD75 step were analyzed on a 15% SDS-PAGE gel. Fractions containing protein were pooled, concentrated to 13.0 mg/mL, and stored at -80°C.

7. RelB DD (277-391) pET15b Mutants

Expression and purification of RelB DD Mutants (RelB DD N287D, RelB DD Y300A, RelB DD I335F, RelB DD I286M I335F, and RelB DD Y300F I335F) were performed similar to RelB DD expression and purification except the SD75 step was not performed. Samples were analyzed on a 15% SDS-PAGE gel, concentrated to similar concentration and stored at -80°C.

8. Daxx DHB I (56-144, C58S) GST TEV

The above plasmid was transformed in BL21 DE3 *E.coli* cells. 4L of LB cell culture (Ampicillin: 100 µg/mL) was grown until $O.D._{600}$ reached 0.5, then induced with 1mM IPTG overnight at 16^{o}C. The cell pellet was lyses in lysis buffer (20 mM MES pH 6.5, 250 mM ammonium sulfate, 50 mM Imidazole, 1 mM DTT, 1 mM EDTA, 1 mM PMSF, 5% glycerol, 0.5% sarkosyl acid), and the lysate was loaded on a GST column (pre-equilibrated with lysis buffer) and washed with 10 CV wash buffer (lysis buffer without sarykosyl acid), and eluted with 10 mM glutathione (in lysis buffer) in 1.5 mL fractions. Fractions were pooled and concentrated to 5 mL to further purify on SD200 size exclusion column using gel filtration buffer (200 mM MES pH 6.5, 250 mM

ammonium sulfate, 50 mM Imidazole, 5% glycerol). Peak protein fractions were pooled, concentrated to 2.14 mg/mL, and stored at -80°C.

9. Daxx DHB II (178-389) GST TEV

The expression and purification were performed similar to Daxx (56-144, C58S) GST TEV except the SD200 step was not performed. Peak fractions were analyzed on 10% SDS-PAGE gel, pooled, concentrated to 1.60 mg/mL, and stored at -80°C.

10. Daxx (60-400) GST TEV

The expression and purification were performed similar to Daxx (56-144, C58S) GST TEV except the SD200 step was not performed. Peak fractions were analyzed on 10% SDS-PAGE gel, pooled, concentrated to 0.68 mg/mL, and stored at -80°C.

11. *N*-Terminal GST-Daxx (1-400) pGEX

The expression and purification were performed similar to Daxx (56-144, C58S) GST TEV except the SD200 step was not performed. Peak fractions were analyzed on 10% SDS-PAGE gel, pooled, concentrated to 1.97 mg/mL, and stored at -80 °C.

C. GST Pulldown Assay

1. Daxx GST with RelB, p50, and RelB/p50 Heterodimer

20 μg of Daxx GST protein and 10 μg RelB, p50, or RelB/p50 Heterodimer were added to 300 μl GST pulldown buffer (20mM tris pH 7.5, 150 mM NaCl, 1 mM DTT, 0.5% Triton X, 0.5 mM EDTA) in a 1.5ml microfuge tube and mixed at 25 °C for 30 min with

shaking. GST beads (pre-equilibrated with GST pulldown buffer) were added to the tubes (15 µl slurry to each tube) and the tubes were incubated for an additional 30 min at 25 °C with shaking. Samples were centrifuged at 10,000xg for 3 minutes in a microcentrifuge. The supernatant was aspirated off and the beads were washed with GST pulldown buffer five times. 5 µl of 4x SDS dye (240mM tris pH 6.8, 40% glycerol, 8% SDS, 0.04% bromophenol blue, 400 mM DTT) was added to each sample, and 15 µl of each sample was loaded on a 10% SDS-PAGE gel.

D. Expression, Purification, and Analysis of His-Daxx:His-RelB Complex

1. Co-Expression Check of RelB RHR (1-400) pET24d with Various Daxx (56-144, C58S) Constructs

The above plasmids were co-transformed in BL21 DE3 *E.coli* cells. 10 mL of LB cell cultures (Kanamycin: 35 µg/mL; Ampicilin: 100 µg/mL) were grown for each sample until $O.D._{600}$ reached 0.2. 1 mL of uninduced sample was saved while, for the remaining samples, 1 mM IPTG was added and the proteins were induced for 3 hours at 37°C. 1 mL from each sample (both induced and uninduced) was taken and centrifuged at 16,100 xg for 1 min at room temperature in a microcentrifuge. The supernatant was aspirated off and the pellet was resuspended in 200 µl lysis buffer (200mM NaCl, 20 mM tris pH 7.5) and sonicated using microsonicator on ice at 30%, cycle 3, for 15 seconds, for three times with 1 min rest. The samples were spun at 16,100 xg for 10 min at 4^oC. The supernatant (soluble fraction) was transferred to new tubes while the pellet (insoluble

fraction) was resuspended in 200 µl lysis buffer. 50 µl of 4x SDS dye was added to both samples and 15 µl was loaded on a 15% SDS PAGE gel. To further optimize the co-expression, similar procedures were performed similar to before except cells were induced with different IPTG concentrations at 16 °C overnight. Samples were analyzed on a 15% SDS-PAGE gel.

2. Co-Expression and Purification of RelB RHR (1-400) pET24D, Daxx (56-144, C58S) pET21d TEV

Based on the expression check condition from above, each plasmid was transformed in BL21 DE3 *E.coli* cells. Cell cultures in 4L LB media (Kanamycin: 35 µg/mL; Ampicillin: 100 µg/mL) were grown till $O.D._{600}$ reached 0.2 and induced with 1 mM IPTG at 16 °C overnight. Protein purification steps were done in a similar manner as in Human Daxx (1-400) pGEX, Murine RelB RHR (1-400) pET24d purification procedures until the Ni^{++} step. Lysis buffer contained 20 mM tris pH 8.0, 1 M NaCl, 10% glycerol, 5 mM βME, 5 mM Imidazole, and 1% sarykosyl acid. Wash buffer contained lysis buffer without sarykosyl acid plus 25 mM Imidazole. Elution buffer contained lysis buffer without sarykosyl acid plus 250 mM Imidazole. Samples were analyzed on a 15% SDS-PAGE Gel. Peak fractions were pooled and concentrated to 1 mL to further purify on an SD200 gel filtration column. Gel filtration buffer (200 mM NaCl, 20 mM tris pH 7.5, 10% glycerol, 1 mM DTT) was used to purify the complex. Peak fractions were analyzed on a 15% SDS-PAGE gel.

3. Western Blot Analysis

The peak fractions from the SD200 gel filtration step were analyzed on a 15% SDS-PAGE gel which was then transferred to an immobilion membrane at 25 V for 1 hour. The membrane was blocked with I-block for 1 hour at room temperature with shaking. His_5-HRP conjugate primary antibody in I-Block (1:10,000) was added to the membrane and blotted for 1 hour at room temperature with shaking. The membrane was washed with TBS-T (25 mM tris pH 7.5, 140 mM NaCl, 0.1% Tween-20) buffer for three times for 10 min each time. Enhanced chemiluminescence reagents were added to the membrane for 2 minutes at room temperature. Then the membrane was developed using BioRad Western Developer.

III. Results

A. The *N*-Terminal Region of Daxx and RHR of RelB Form a Complex *in vitro*.

Since Puto *et al.* have shown than Daxx and RelB interact with each other *in vivo* to achieve transcriptional repression, the first focus of the study was to see if this happens *in vitro* as well. In order to achieve this goal, the *N*-terminal region of Daxx (1-400), a generous gift from Lorena Puto, was co-expressed with RelB RHR (1-400) in Rosetta *E.coli* competent cells. Since RelB RHR is in His-tag containing vector (pET 24d) while Daxx *N*-terminus is in GST tag containing vector (pGEX), the purification of the co-expressed protein was performed by first using Ni^{++} resin followed by GST resin. **Figure 11** shows that there was excess RelB RHR when the co-expressed protein was purified through the Ni^{++} column. This is because Daxx *N*-terminus was mostly in the insoluble fraction while more RelB RHR was in the soluble fraction. GST-tagged Daxx *N*-terminus band on SDS-PAGE gel had three different bands in close proximity, and it is observed that the middle band remained mostly insoluble. The interaction, however, became 1:1 ratio after passing through the GST column. **Figure 12** shows that most of RelB RHR came out in the flow through and wash. The first wash had more RelB RHR while second wash had almost no protein. Daxx, in the elution fractions, had multiple bands like in **Figure 11**. This suggests that the three bands from **Figure 11** were not products of degradation, but non-specific bands since, after passing through GST resin, the number of bands near Daxx decreased from three to two. The fact that RelB RHR still was eluted together with *N*-terminal GST-tagged Daxx suggests that the interaction between these

two *N*-terminal regions of Daxx and RelB is strong. Since RelB RHR has no affinity to GST resin, yet after passing the co-expressed protein to GST resin, RelB RHR was eluted with Daxx *N*-terminus. This means that these two proteins have strong affinity to each other *in vitro* as well. The last wash fraction shows that there was barely any unwashed protein left. Yet, once 10 mM glutathione was added, more protein complex came off. This confirms that the protein elution fractions were as a result of binding and not as a result of insufficient washing of the GST resin. Finally, after the elution fractions from **Figure 12** were concentrated, two prominent bands showed up on SDS-PAGE gel analysis in **Figure 13**. The concentrated complex shows that, while Daxx had some degradation products under its size, RelB RHR is more stable than Daxx *N*-terminus. Yet the presence of the intense bands corresponding to Daxx:RelB *N*-terminus confirms that the Daxx:RelB *N*-terminus complex can be expressed and purified successfully *in vitro*.

B. p50 RHR and RelB RHR Can Be Denatured and Refolded to form p50:RelB.

In order to form p50:RelB RHR complex, Moorthy *et al*. have already devised protocols that involve denaturing and refolding of the individually purified p50 RHR and RelB RHR proteins. **Figure 14** shows the purification of p50 RHR. Around 200 mM NaCl, p50 RHR was eluted. Although some protein was observed in the flow through, this was probably due to the fact that p50 RHR has a low pI, so using a buffer with lower pH would have helped make the proteins more positively charged, thus increasing binding affinity to the S column. **Figure 15** shows p50 DD purification, which was

cleaner than the p50 RHR purification. This was probably because of the fact that a wider gradient was used, thus allowing more fractions to be collected which would have helped with the overall protein purity. Concentrated p50 DD shows that the purification was very successful. **Figure 16** shows RelB RHR purification samples. The insoluble sample had a majority of the protein, while the flow through fraction had little protein. This suggests that denaturing the protein would have increased the yield since RelB RHR has strong affinity to Ni^{++}. Concentrated protein shows clean protein. After RelB RHR and p50 RHR were individually purified, they were denatured in the presence of 8 M urea and then slowly refolded to native state by dialyzing against urea-free buffer. This slow dialysis was very important to ensure that the complex did not precipitate. Also, during the process of denaturing, the proteins had to be in a fairly dilute condition (0.36 mg/mL) which was important because if the concentration was too high, the proteins might not have enough free space to move around and form a heterodimer. No precipitated protein was observed during this process which suggests that the complex formation was very stable. After the complex was made, it was diluted to low salt buffer to bind HiTrap S column for further purification. **Figure 17** shows that when p50 RHR and RelB RHR heterodimer was made and purified over HiTrap S column, the affinity and binding to S column was very strong, which allows purification of highly pure heterodimer with 1:1 protein ratio.

C. Daxx *N*-Terminus Interacts Specifically with RelB RHR and RelB DD.

Figure 23 shows purification of Daxx *N*-terminus. Although the yield was greater than that of DHB II, there were more degradation products in this preparation than other Daxx constructs. Since the purpose of this protein was for GST pulldown, having a prominent band at a correct size was sufficient to proceed to the next step. GST pulldown was performed because Daxx has a GST tag while RelB and p50 do not have GST tags. Based on GST pulldown analysis, **Figure 25** shows that Daxx *N*-terminus has a strong binding affinity to RelB RHR, but not to p50 RHR. Although **Figure 25** does not show the binding of RelB DD to Daxx *N*-terminus, future studies will hope to prove that under denaturing conditions with RelB DD, binding does occur with Daxx *N*-terminus. GST controls, which are the combination of GST protein and other variable proteins, show that there was no non-specific binding to GST protein (**Figure 30**). The most remarkable finding is that p50:RelB RHR heterodimer did not bind to Daxx *N*-terminus when the p50:RelB RHR pre-formed heterodimer was added. This means that when the pre-formed p50:RelB RHR complex was added, Daxx could not disrupt this binding because the binding between p50:RelB RHR had already been formed prior to the addition of Daxx. Since the p50:RelB RHR complex was made through denaturing the proteins in 8M urea and slowly refolding, the complex is thought to be tight and strong. However, when RelB RHR and p50 RHR were separately added to Daxx *N*-terminus, the binding of RelB RHR and Daxx *N*-terminus reappeared (**Figure 26; Figure 28).** This means that Daxx has affinity for binding to RelB in native state, but p50 can compete out with this binding. This also hints to the fact that in normal resting state, most cells have p50:RelB RHR heterodimer complex that triggers the survival pathway of NF-κB. But under cellular stress and apoptotic signal, Daxx competes out this binding of RelB:p50 by binding to

RelB before p50 can bind, triggering DNA methylation as RelB has DNA binding domain to induce cell death in association with Dnmt (DNA methyl transferase). **Figure 29** shows that although previously Daxx *N*-terminus did not seem to bind to RelB DD, under denaturing condition with 3M urea, RelB DD was more opened up which allowed for better binding to Daxx *N*-terminus.

D. Daxx DHBI + II Interacts Specifically with RelB RHR and RelB DD.

Figure 22 shows the purification of Daxx 60-400 which was similar to that of DHB II. **Figure 25** shows that Daxx 60-400, which is nearly identical to Daxx DHB I and DHB II, did bind strongly to RelB RHR as Daxx *N*-terminus does. p50 RHR, however, did not bind to any part of Daxx *N*-terminus while RelB DD binding was not significant. In all the pulldown experiments, GST controls were performed to ensure that there was no non-specific bonding of RelB and p50 to GST protein (**Figure 30**). Since Daxx (60-400) included both Daxx DHBI and Daxx DHBII, even though it was previously shown that Daxx DHBII did not interact with RelB, because of the presence of Daxx DHBI in Daxx 60-400, the binding to RelB still occurred as expected.

E. The *N*-Terminus DHBI Domain of Daxx is Sufficient in Mediating the Interaction with RelB RHR and RelB DD.

In order to fine tune the domain requirement for binding, Daxx DHBI was tested for its binding affinity to RelB and p50. **Figure 24** shows Daxx DHBI bound to RelB RHR very strongly and slightly to RelB DD, but not to p50 RHR (**Figure 32**). **Figure 27**

shows that Daxx DHBI bound very strongly to RelB RHR even when p50 DD was trying to compete out the binding. As previously seen in Daxx *N*-terminus, the pre-formed p50:RelB RHR complex did not bind with Daxx DHBI while RelB RHR itself did bind very strongly with Daxx DHBI (**Figure 28)**. This means that Daxx DHBI is important and sufficient for binding to RelB RHR in the same way as Daxx *N*-terminus bound to RelB. Finally, **Figure 29** shows that under native versus denaturing conditions, the binding of Daxx DHBI and RelB DD was more enhanced in the denaturing condition than the native condition (**Figure 31).**

F. Daxx DHBII Does Not Interact with RelB.

The purified Daxx DHBII was used for GST pulldown analysis. **Figure 21** shows that while the yield was not satisfactory, protein purity was relatively clean and acceptable for GST pulldown analysis. Unlike Daxx *N*-terminus or Daxx DHBI, Daxx DHBII did not interact with any RelB or p50 construct (**Figure 24**) like those of its GST controls (**Figure 30**). This is interesting because even though it was found that the *N*-terminal region of Daxx and Daxx DBHI had strong interaction with RelB RHR, Daxx DHBII was completely different. The fact that Daxx DHBII behaved in a very different way for binding to RelB than Daxx DHBI hints that Daxx DHBI, and not Daxx DBHII, is sufficient for binding to RelB.

G. Daxx DHBI Binds Differently to RelB DD Defective Mutants

Since it was found that the smallest domain organization for binding between Daxx and RelB was Daxx DHBI and RelB DD, further pulldown analysis with RelB DD was performed. First, **Figure 18** shows the purification of RelB DD, which came out soluble and pure. Even though there was a small band slightly above RelB DD (13kDa), after gel filtration, only RelB DD was left. Finally, **Figure 19** shows purification of different RelB DD mutants. Most of the proteins were highly soluble, yet a lot came out in flow through. This is possibly due to the fact that RelB DD mutants change the dimerization domain interface of RelB DD which might have affected their affinity to the Ni^{++} resin. Finally, **Figure 32** shows changes in binding differences between RelB DD WT and RelB DD mutants to Daxx DHBI. In particular, RelB DD N287D enhanced the binding to Daxx DHBI while RelB DD Y300A had similar level of binding affinity to Daxx DHBI as RelB DD WT. Other mutants such as RelB DD I335F, RelB DD I286M, I335F, and RelB DD Y300F, I335F, however, had no binding to Daxx DHBI. These mutants, which did not bind to Daxx DHBI, are mutants that were generated to resemble p50 dimerization domain interface, which is known to have the strongest dimer affinity in NF-κB. Since these mutants were encouraged to have stronger dimer domain interaction, they would form tighter homodimers than the wild-type, resulting in less affinity to Daxx DHBI binding. The fact that mutants in RelB DD changed the binding affinity with Daxx DHBI hints that RelB DD has specific affinity to Daxx DHBI, although one mutant (RelB DD N287D) seemed to increase the binding significantly. But this is probably because RelB DD N287 is not participating in the core dimerization interface site. In order to better understand the relationship between RelB DD dimer structure and binding to Daxx DHBI, mutant RelB DD needs to be expressed, purified, and crystallized.

H. Daxx:RelB Complex is Weak.

Having shown that Daxx DHBI binds specifically to RelB RHR and RelB DD, the complex purification of Daxx:RelB was performed. It was surprising, however, that Daxx DHBI and RelB DD co-expressed complex was unstable as the proteins kept precipitating during the purification process. Daxx DHBI and RelB RHR, however, was more stable than that of RelB DD, as the co-expression of RelB RHR and Daxx DHBI in His-tagged vectors were successful. Based on the result from **Figure 33**, it was found that Daxx DHBI in His-tagged or non-tagged vector co-expressed with RelB RHR in His-tagged vector had the highest expression. But the expression was mostly in the insoluble sample. For that reason, more variations with IPTG induction level and temperature change were performed to better optimize protein expression (**Figure 34**). Based on the result, it was found that Daxx DHBI in His-tag co-expressed with RelB RHR in His-tag had the best expression. **Figure 35** shows that the co-expressed proteins can be purified by passing through Ni^{++} column. However, **Figure 36** shows that when the proteins from Ni^{++} column were further separated through the size exclusion chromatography, the interaction was dismantled, and only the individual proteins at different sizes were eluted. **Figure 37** confirms this finding by showing that there was only one band that was recognized by His antibody which corresponded to RelB while Daxx was picked up in later fractions where the size did not correspond to the theoretical complex size with RelB.

IV. Discussion

A. Daxx DHBI is Sufficient for Binding to RelB DD.

This study provides two important insights into the mechanism of Daxx:RelB complex function. First, Daxx:RelB formation is independent of NF-κB since RelB:p50 heterodimer does not interact with Daxx *N*-terminus whereas free RelB RHR does. This suggests that the interaction between Daxx and RelB is not dependent on the dimerization of RelB with other NF-κB factors such as p50 or p52. This also provides insights about the binding mechanism of the Daxx:RelB complex. The inability of the RelB:p50 heterodimer to bind Daxx suggests that perhaps the domain interface of RelB is directly involved in Daxx binding. Since the dimer interaction site is occupied in the RelB:p50 heterodimer, Daxx cannot contact RelB. But when each protein RelB RHR and p50 RHR is added to Daxx, a specific Daxx:RelB complex is formed. The fact that RelB DD binding is diminished when p50 DD is added, compared to RelB DD alone added to Daxx, suggests that Daxx and p50 compete for an overlapping binding site in RelB. This notion is further supported by Daxx's interaction with RelB dimerization mutants. Our laboratory has generated several RelB mutants that show altered dimerization with itself or with p50 and p52. Five of these mutants are used in this study: RelB DD N287D; Y300A; I335F; I286M, I335F; and Y300F, I335F. The last three mutants bind poorly to Daxx. These residues are critical for RelB heterodimer formation. RelB N287D is highly defective in heterodimer formation but shows enhanced binding to Daxx. Since both p50 and p52 contain an Asp at the homologous position, an Asp-Asp pair is detrimental to RelB:p50/p52 dimerization. However, Asp mutant may make contact with Daxx further

suggesting a role of the dimer interface in Daxx binding. In all, these results suggest that RelB is at the center of two diverse physiological functions: one in association with its well known NF-κB partners and the other role is in association with Daxx. Interestingly, NF-κB-dependent activity is pre-dominantly related to cell survival where Daxx associated activity of RelB is linked to cell death.

B. Daxx:RelB might be a Part of a Multi-Protein Complex

Although GST Pulldown assay confirmed interaction between Daxx DHBI and RelB DD, the Daxx DHBI:RelB RHR complex was not able to be purified as a single complex by size-exclusion chromatography. This suggests a specific but weak interaction between these two proteins. Even though it was already shown that Daxx and RelB RHR have a higher binding affinity where the complex can be purified, because it is shown that Daxx DHB II does not play any role in binding capability with RelB RHR, the experiment focused more on purifying Daxx DHB I with RelB RHR instead of the entire Daxx *N*-terminus. Since Daxx DHBI:RelB DD complex was much weaker than that of Daxx DHBI:RelB RHR, RHR of RelB was used to form a complex with Daxx DHBI. Thus, while it is still possible that Daxx *N*-terminus and RelB RHR complex might be easier to purify and form a complex, more attention was paid to Daxx DHB I to better elucidate the binding behavior of Daxx to RelB in this study.

The difference between GST pulldown result and size exclusion chromatography result is possibly due to the weak binding affinity of the Daxx:RelB complex. Complexes with K_D value as high as 10 μM can survive gel filtration suggesting that the affinity of

the complex is lower than 10 μM. GST pull down assay can detect binding for complexes with even lower affinity, in the range of mM, and since the proteins are concentrated on the beads, binding can be observed. Thus the interaction between Daxx DHB I and RelB RHR was good enough to be analyzed via GST pulldown assay, but not via gel filtration method. This prevented the complex from being isolated for structural studies. This raises an interesting question which is how these two proteins with such weak binding remain as a complex *in vivo*. One possibility is that they interact strongly upon specific modification and/or when they are part of a larger protein complex *in vivo*. Since Daxx interacts with Dnmt (DNA methyl transferase), chromatin medicating complex might be involved to strengthen the interaction between Daxx and RelB, which is a subject of future studies. In addition, understanding the dimerization domain behavior of other RelB mutants can add more insight about the dimerization mechanism of RelB and their effect on interaction with Daxx.

V. Conclusion

The main purpose of this study was to elucidate the domain organization of Daxx and RelB that are essential and sufficient for binding to each other *in vitro*. This goal was based on a previous finding that Daxx and RelB interact strongly *in vivo*. In order to achieve this purpose, molecular cloning on different domains of Daxx and RelB were performed. Based on a previous finding that Daxx *N*-terminus is composed of two main helical bundles (named as DHBI and DHBII), Daxx *N*-terminus, Daxx DHBI, and Daxx DHBII were tested for binding affinity using GST pulldown with RelB and p50. The most important finding was that when RelB:p50 RHR pre-formed complex is added to Daxx *N*-terminus, there is no binding, but when RelB and p50 are added separately to Daxx *N*-terminus, Daxx *N*-terminus specifically binds to RelB. This means that Daxx *N*-terminus has strong preference to bind to RelB RHR, but when the dimerization domain interface is occupied, the binding disappears. Therefore, it makes sense that Daxx binds to RelB DD as well. Finally it was found out that Daxx DHBI and RelB DD are required for binding to each other, but this complex was not feasible to be purified for complex analysis. When Daxx DHBI and RelB RHR were purified through Ni^{++}, the purification was successful until it reached gel filtration step where the complex dissociated. This means that while Daxx DHBI and RelB RHR interact, the interaction is not strong enough since it cannot survive after gel filtration step. This also means that because RelB interacts with p50 or other NF-κB members, the binding affinity between RelB and Daxx is not very strong unless in physiological conditions, external apoptotic stimuli induce tighter binding so that RelB can bind to DNA for Daxx to methylate. But since this study

was done in vitro, it was not possible to understand the cellular mechanism of this binding between Daxx:RelB although this weak binding behavior can be linked to biological significance based on the binding specificity. Future studies of this project can include further elucidating the binding interaction of Daxx:RelB that is feasible for crystallization analysis as well as understanding the structural mechanisms of different RelB DD mutants that can explain how changes in dimerization domain structure can influence the ability of RelB DD in binding to important proteins like Daxx.

Appendix

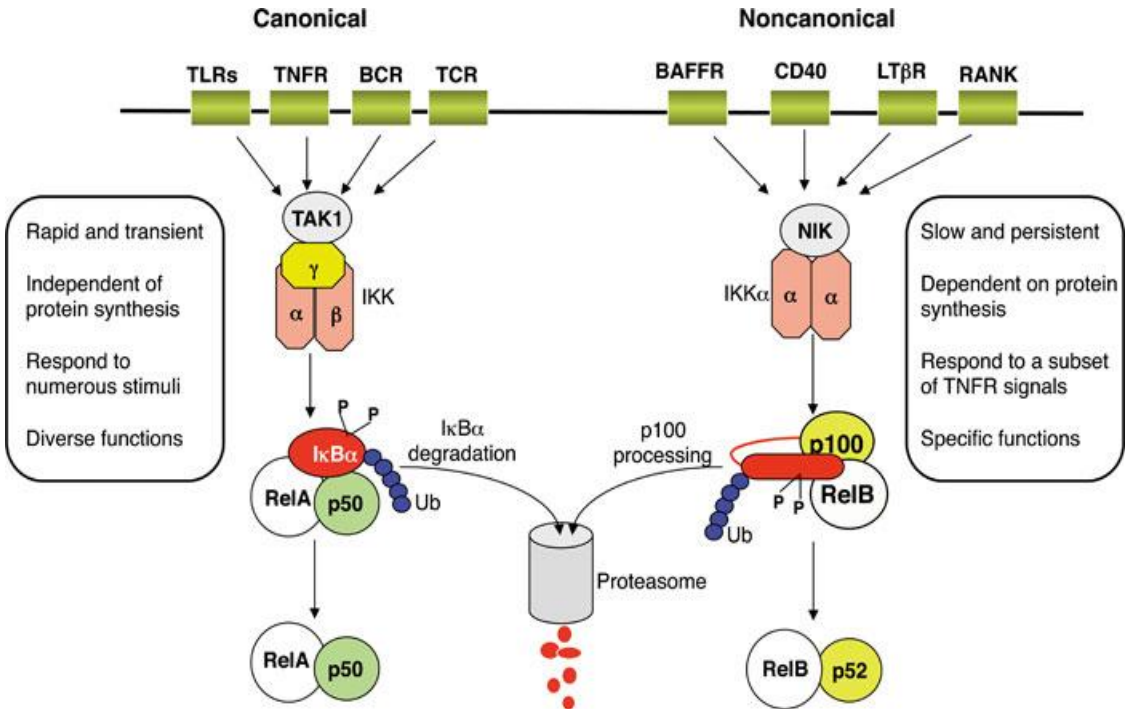

Figure 1: NF-κB Signaling Pathways. The two main singling pathways are canonical and non-canonical. In canonical pathway, IκB is degraded by ubiquitin degradation, releasing RelA:p50 heterodimers inside the nucleus. In non-canonical pathway, p100 serves as IκBγ whichis degradedby ubiquitin degradation while the rest of p100 is processed into p52 that can form a heterodimer with RelB.

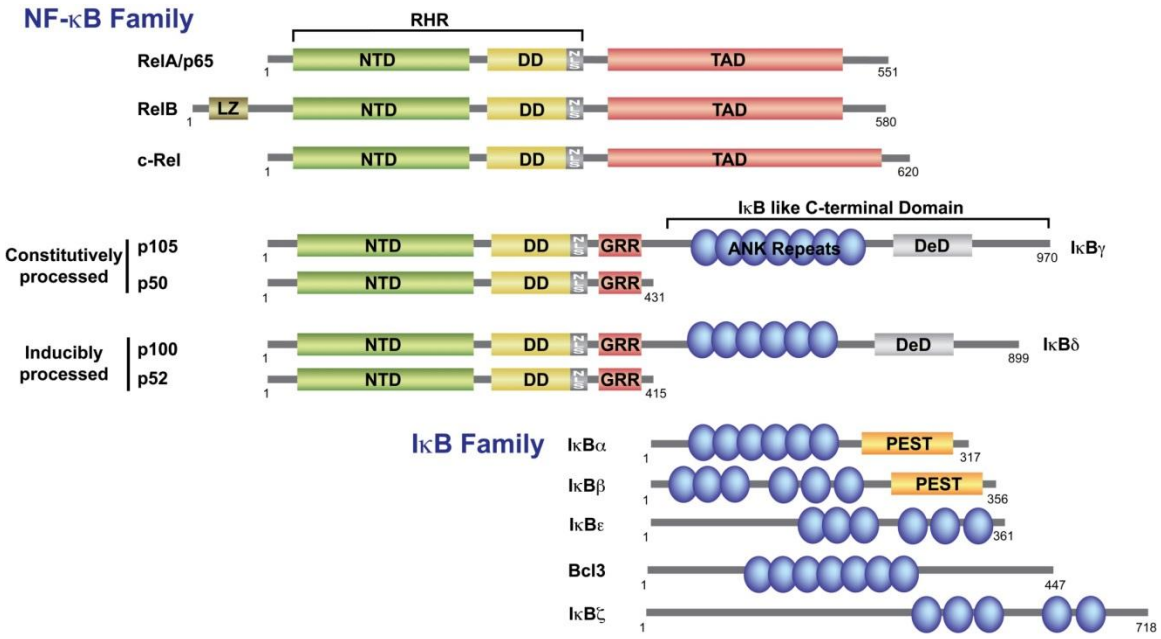

Figure 2: Domain Organization of NF-κB Protein and IκB Protein Family Members. There are five main NF-κB protein members and five IκB members. RelA/p65, RelB, and c-Rel have transactivation domain (TAD) while p105 and p100 have Ankyrin repeat domain (ARD) like IκB members (Wang, 2011).

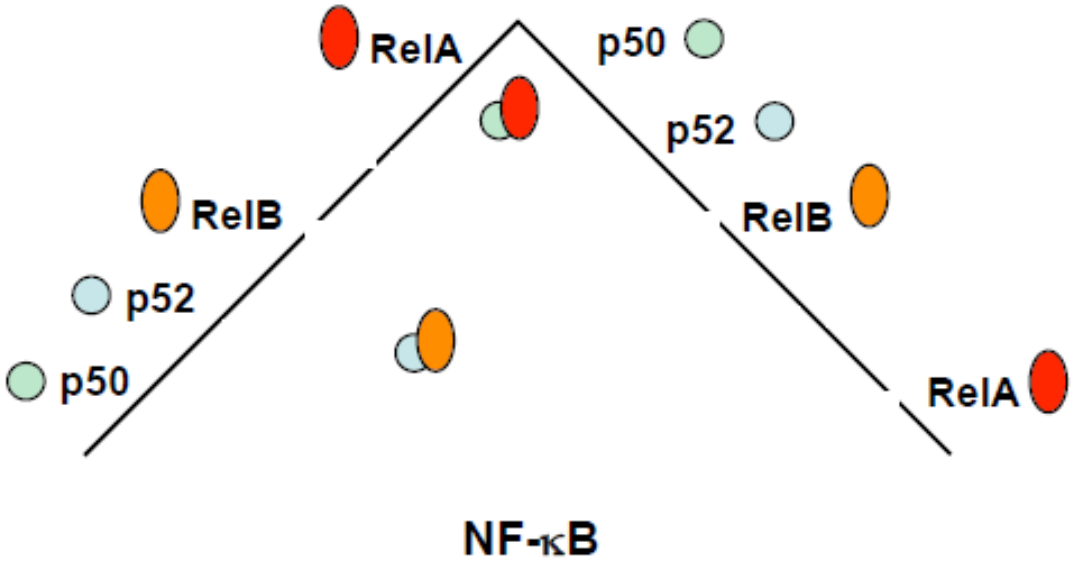

Figure 3: Fifteen Possible Dimers of Multiple NF-κB Dimers. Many different combinations of NF-κB dimmers can form. The main heterodimers are RelA:p50 and RelB:p52. RelA:p50 is prominent in canonical pathway while RelB:p52 is a characteristic of p100 processing, which involves non-canonical pathway (Hoffmann, 2012).

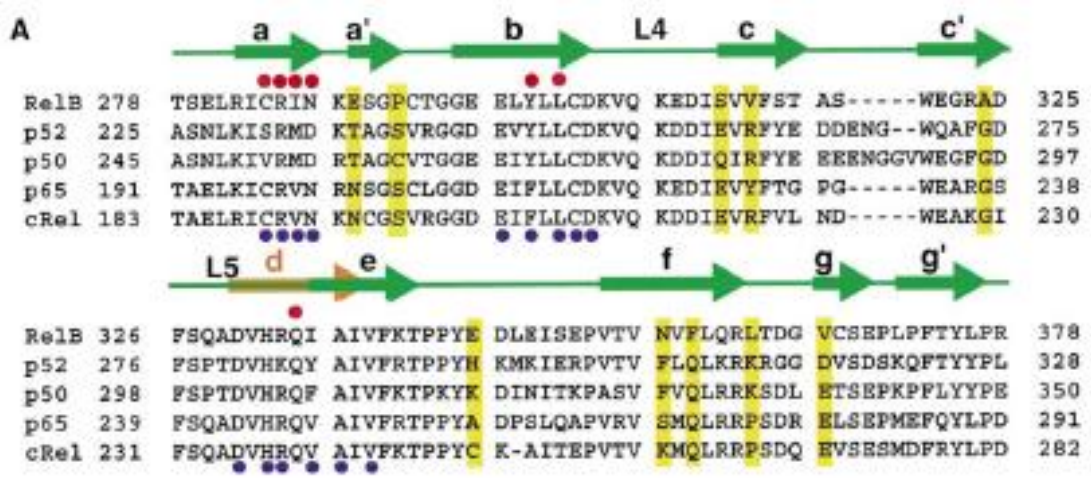

Figure 4: Primary Amino Acid Sequences for Different Murine NF-κB Protein Domains. Five NF-κB members have similar sequence homology that make up different sheets in dimerization domain. These amino acids are important in creating dimerization domain interface of NF-κB (Huang *et al.*, 2005).

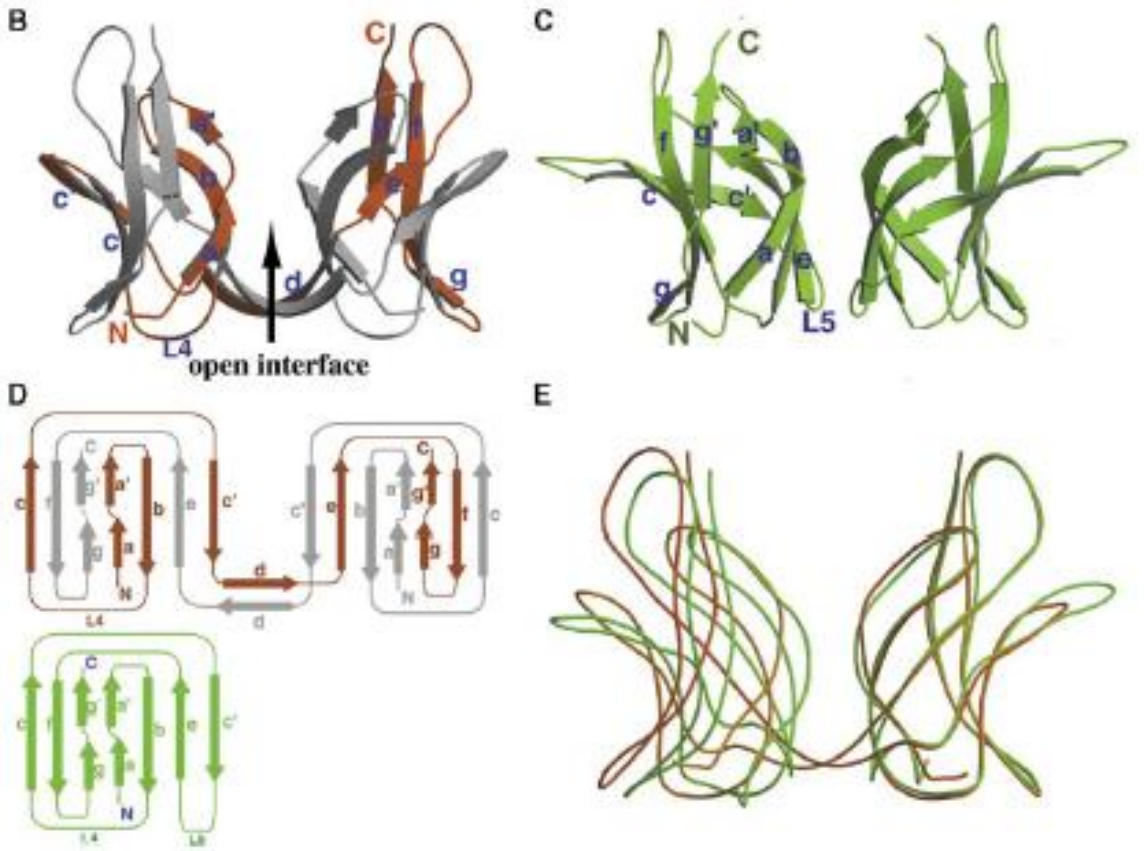

Figure 5: Tertiary Structure of Murine NF-κB Dimerization Domain Proteins. Orange is for RelB DD while Green is for p50 DD. Both dimmers have an open interface which allows for binding of other proteins. p50 DD has tighter binding than RelB DD (Huang *et al*., 2005).

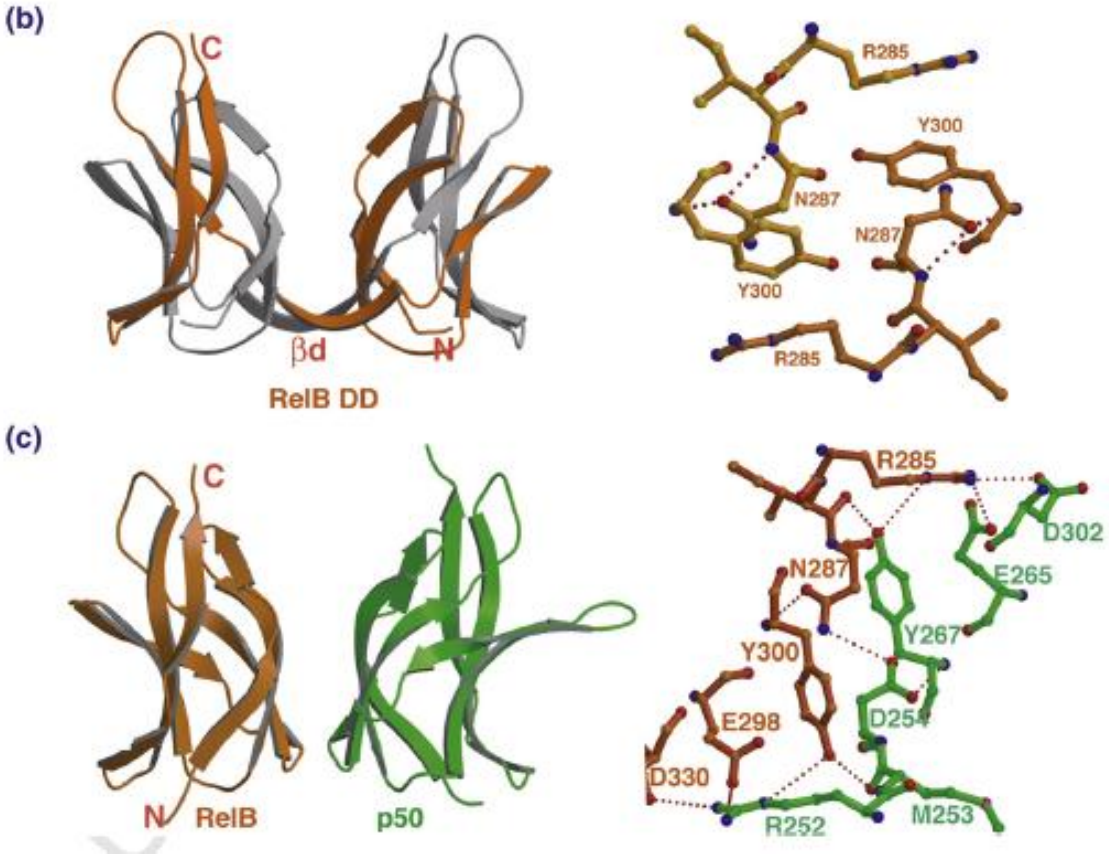

Figure 6: Tertiary Structure of RelB Dimers and RelB:p50 Heterodimer. When RelB:p50 heterodimer is crystallized, different amino acids make different contacts with each other, showing that these are key amino acids that make up the dimerization domain interaction (Vu *et al.*, 2013).

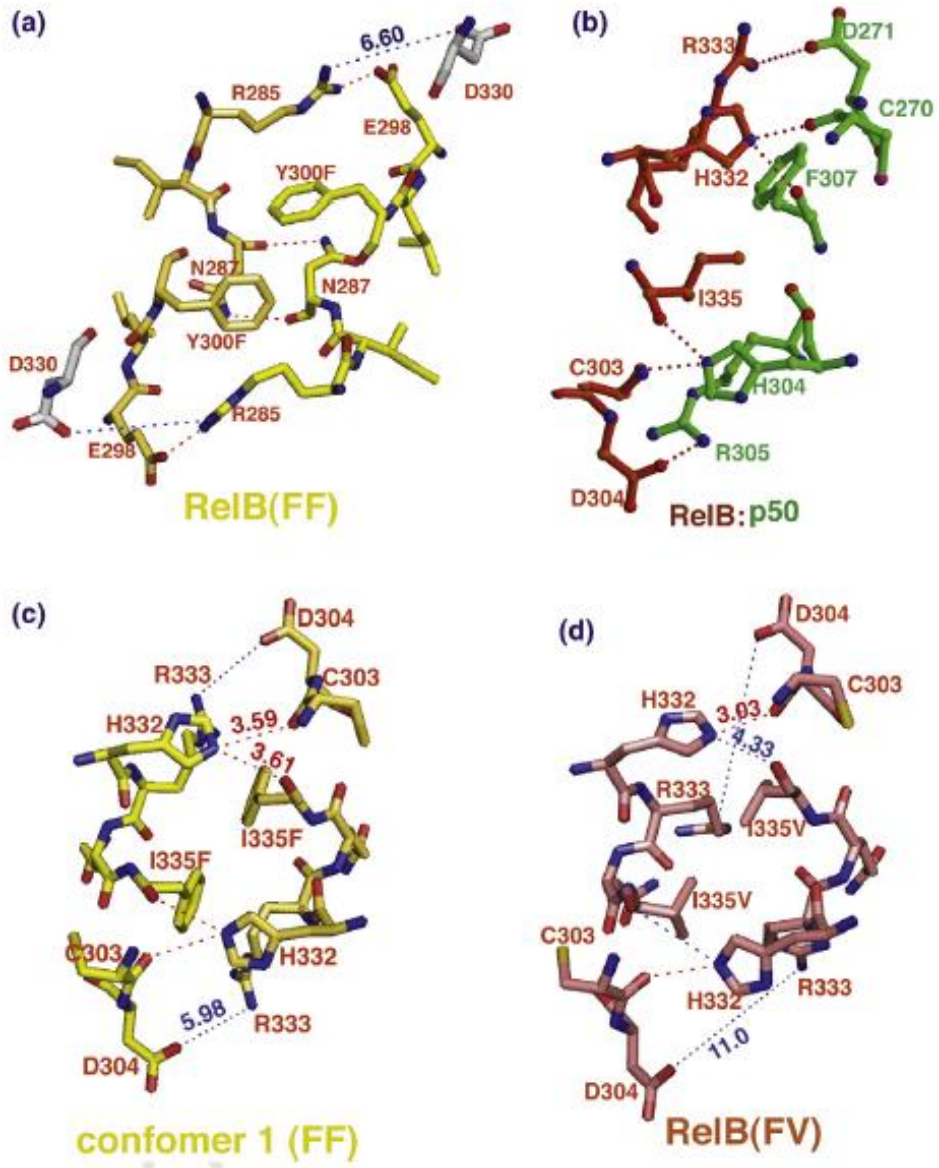

Figure 7: Subunit Interactions of Different NF-κB Dimers and Mutants. When some of the key amino acids of RelB are mutated, the dimerization domain interface is changed, showing that the key amino acids in dimerization domain have the ability to disrupt the domain interface (*Vu et al.*, 2013).

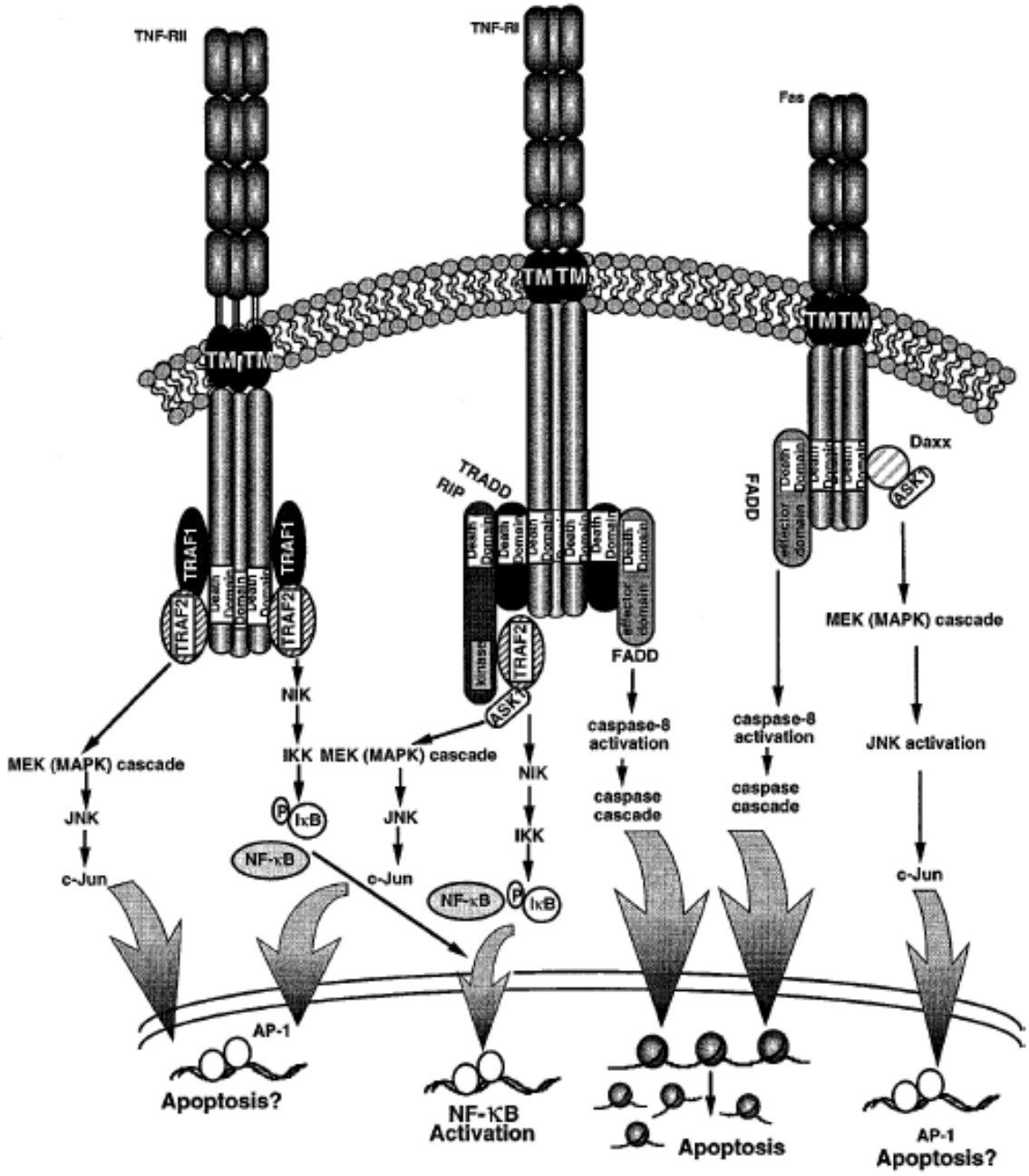

Figure 8: TNF Receptor Pathway and Interaction with Daxx. Daxx is a death-domain associated protein involved in Fas-binding pathway. By triggering JNK pathway, it induces mitochondrial outer-membrane permeabilization (MOMP) response inside the cells upon external apoptotic stimuli (Baker *et al.*, 1998).

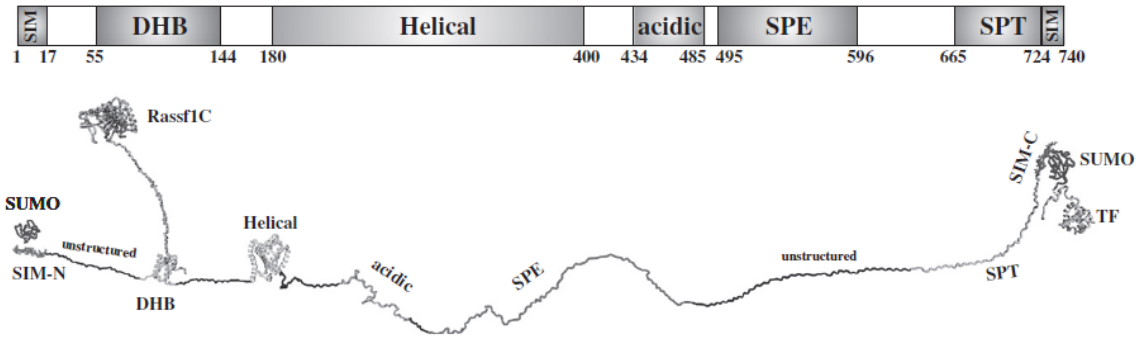

Figure 9: Domain Organization of Daxx Based on Sequence Predictions. The Daxx *N*-terminus is highly structured which contains DHB I (Daxx helical bundle) and II, while the C-Terminal is highly disordered (Escobar-Cabrera *et al.*, 2010).

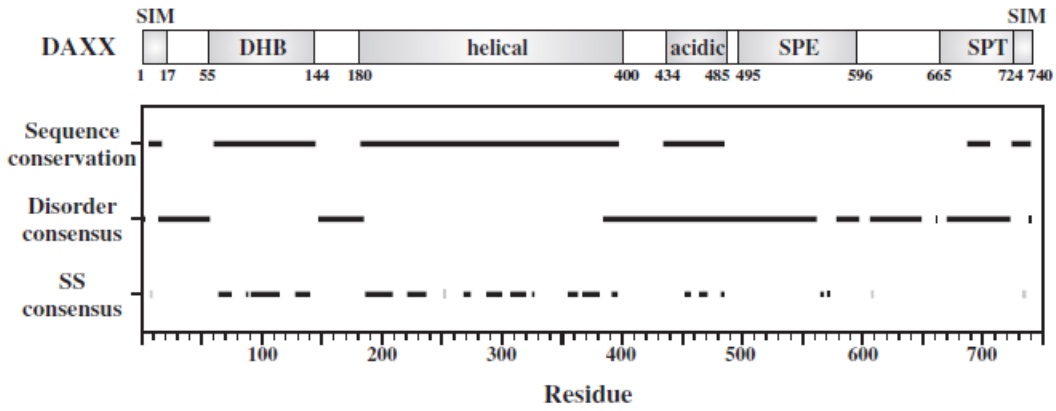

Figure 10: Modular Organization of Daxx Based on Sequence Predictions. The sequence conservation of *N*-terminal region of Daxx is high while the disorder consensus for C-Terminal region is high (Escobar-Cabrera *et al.*, 2010).

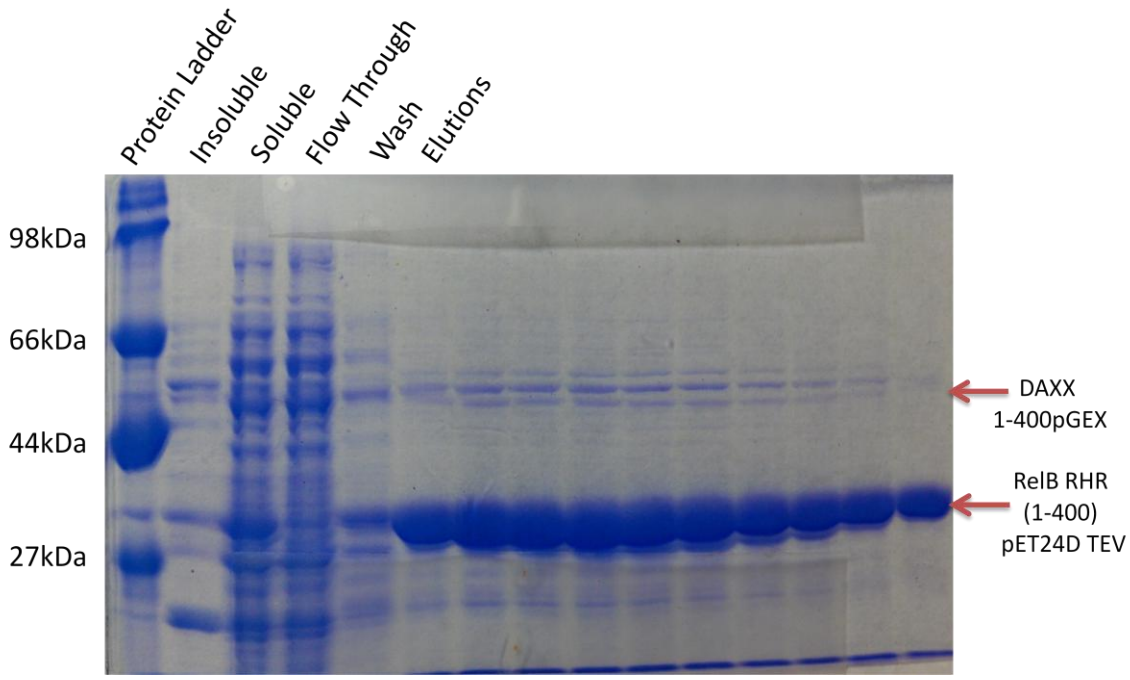

Figure 11 : Purification of Co-Expressed Human Daxx (1-400) pGEX, Murine RelB RHR (1-400) pET24D. 2L LB culture was grown for the cell expressed in Rosetta strain which was later purified via Ni^{++} Column and analyzed on 10% SDS PAGE Gel.

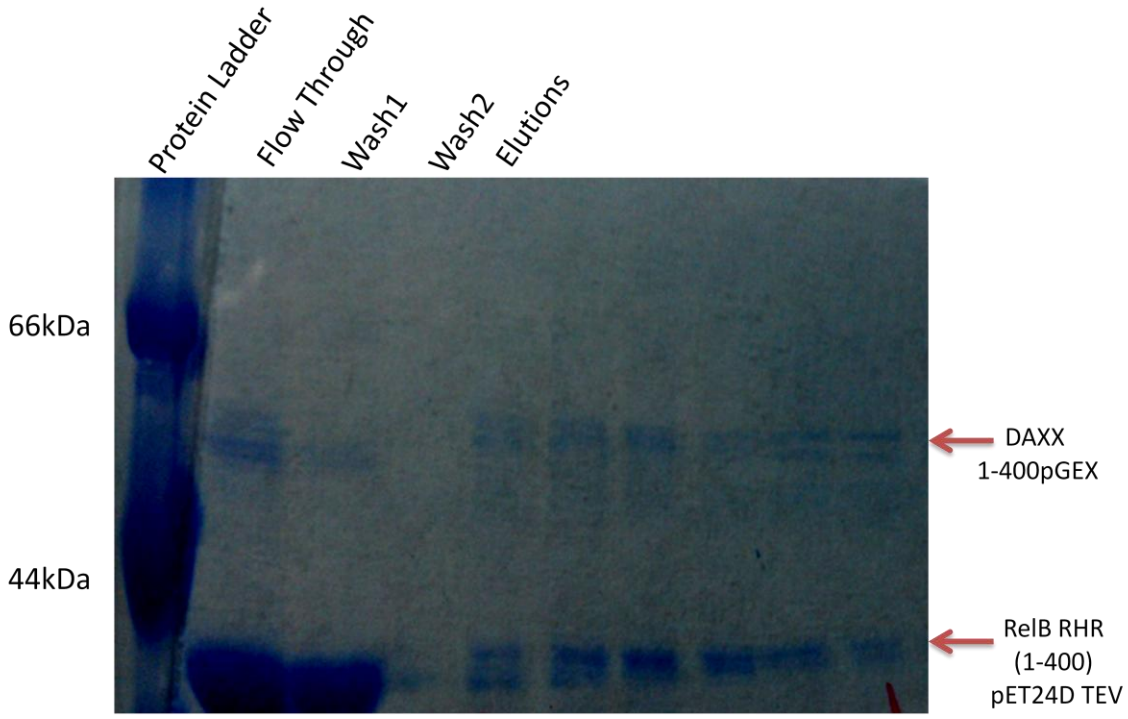

Figure 12: Purification of co-expressed Daxx (1-400) pGEX, RelB RHR (1-400) pET24D. The protein from Figure 11 is further purified by passing through GST colun which is then analyzed on 10% SDS PAGE Gel.

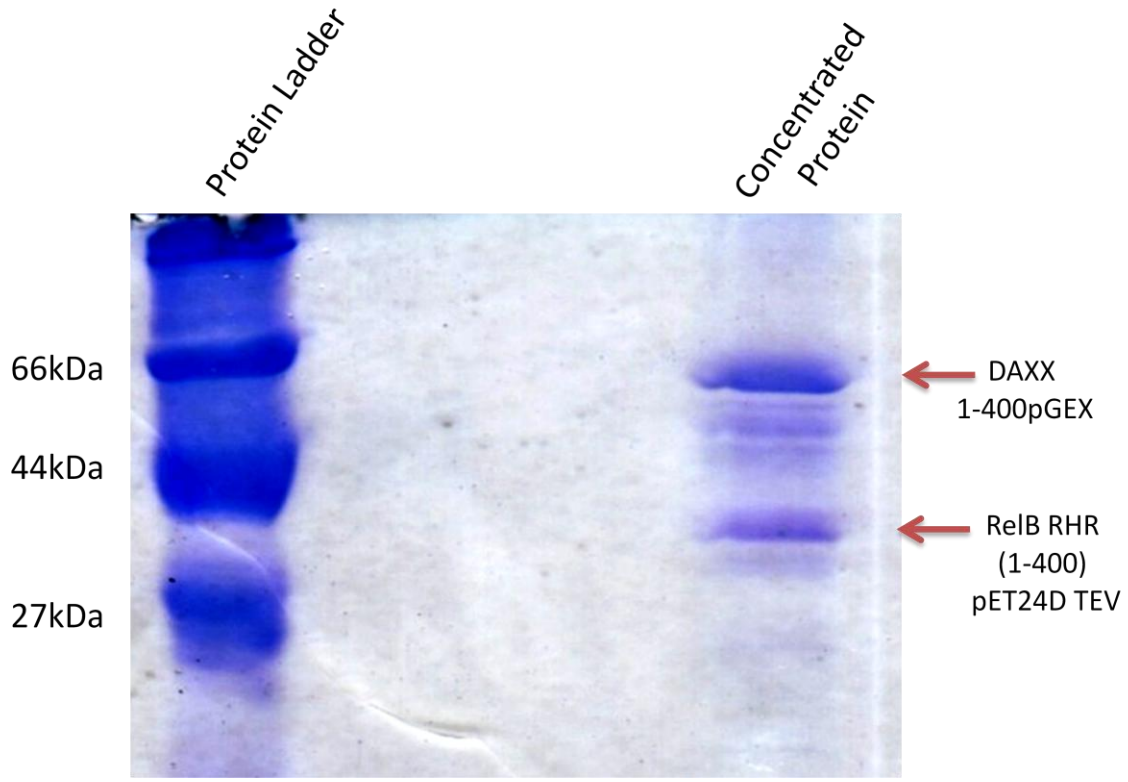

Figure 13: Co-expressed Daxx1-400pGEX, RelB RHR (1-400) pET24D. After purifying the complex through Ni^{++} and GST column, the proteins were concentrated and analyzed on 12.5% SDS PAGE Gel.

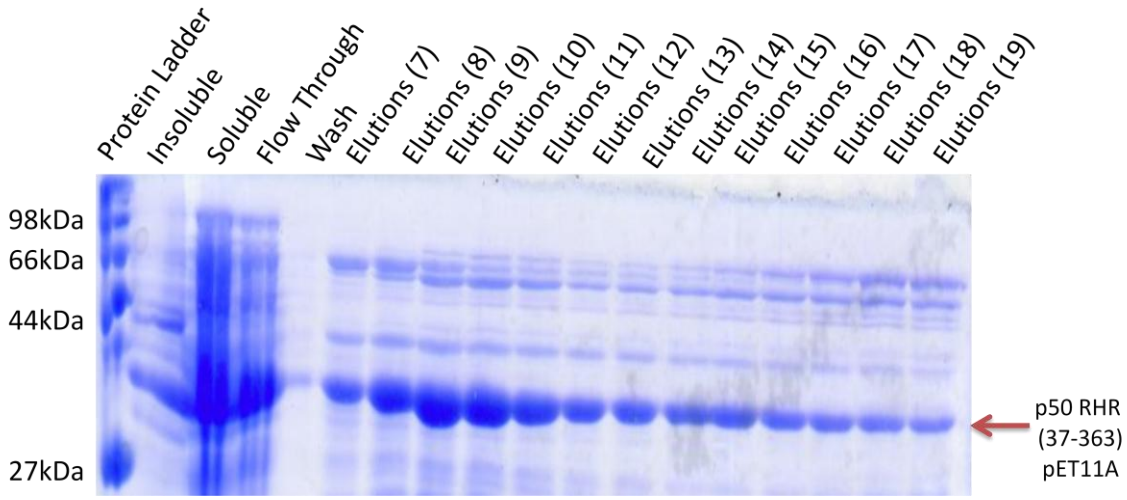

Figure 14: Purification of Murine p50 RHR (37-363) pET11A. Plasmid was expressed in BL21DE3. 2L culture was grown and purified via FastFlowSP Column using NaCl Gradient. Samples are analyzed on 10% SDS PAGE Gel.

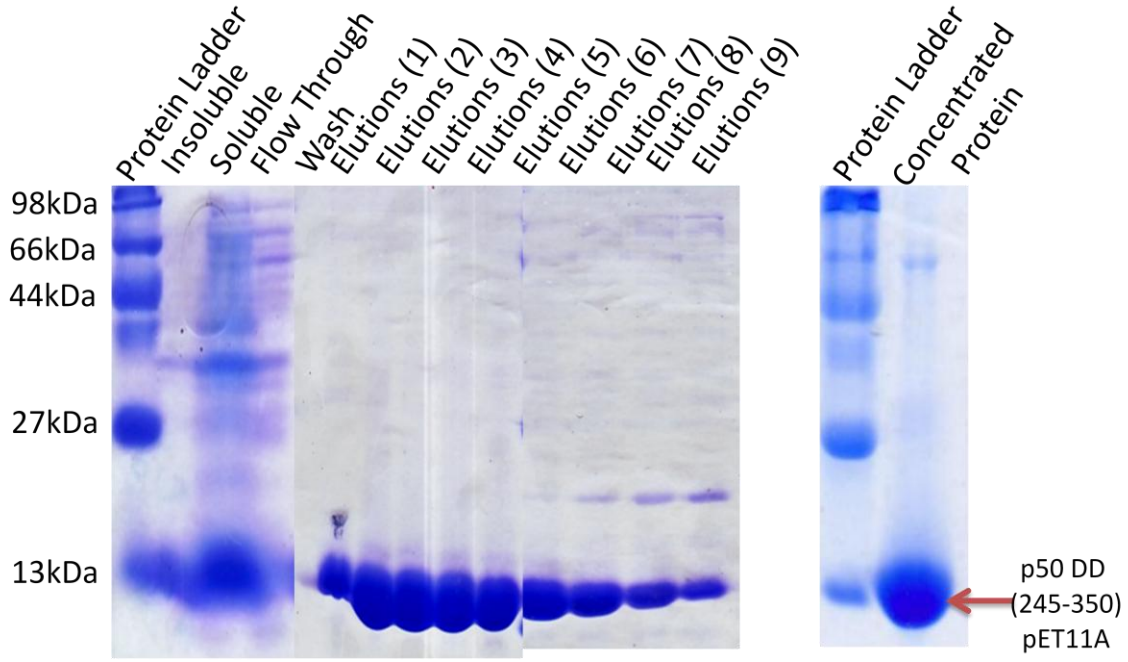

Figure 15: Purification of Murine p50 DD (245-350) pET29B RBS. The plasmid was expressed in BL21DE3. 2L LB media was grown which was then purified using FastFlowSP column using NaCl gradient. Samples are analyzed on 15% SDS PAGE Gel. The concentrated protein shows that protein purification is highly successful.

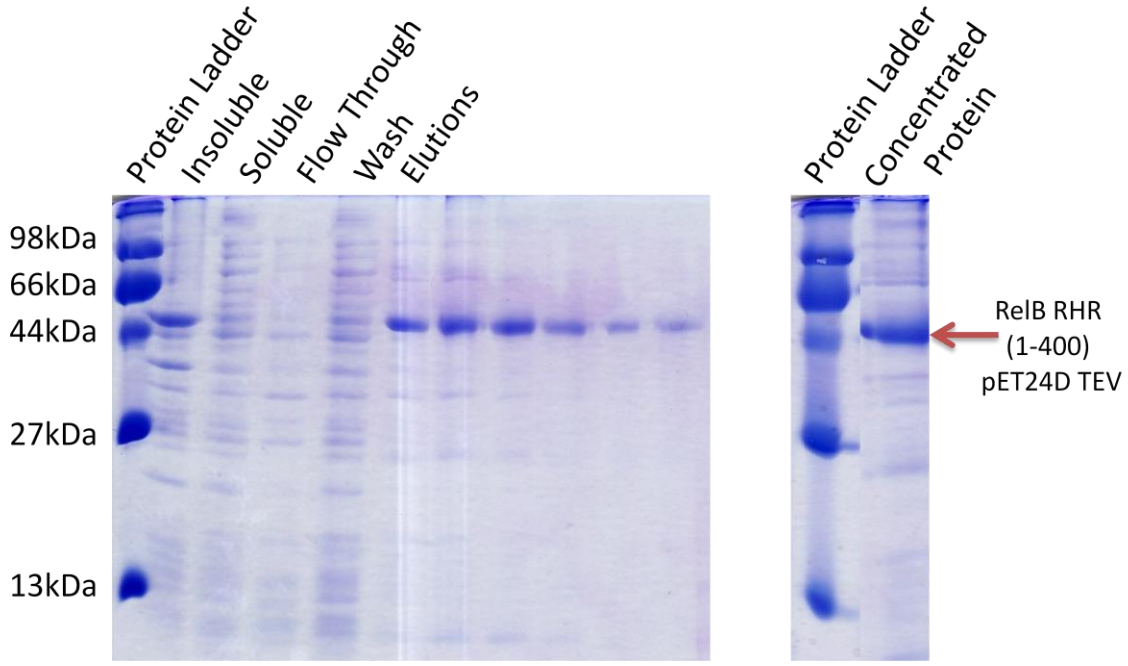

Figure 16: Purification of Murine RelB RHR (1-400) pET24D TEV. Plasmid was expressed in BL21DE3 and purified via Ni^{++} Column which is then analyzed on 12.5% SDS PAGE Gel.

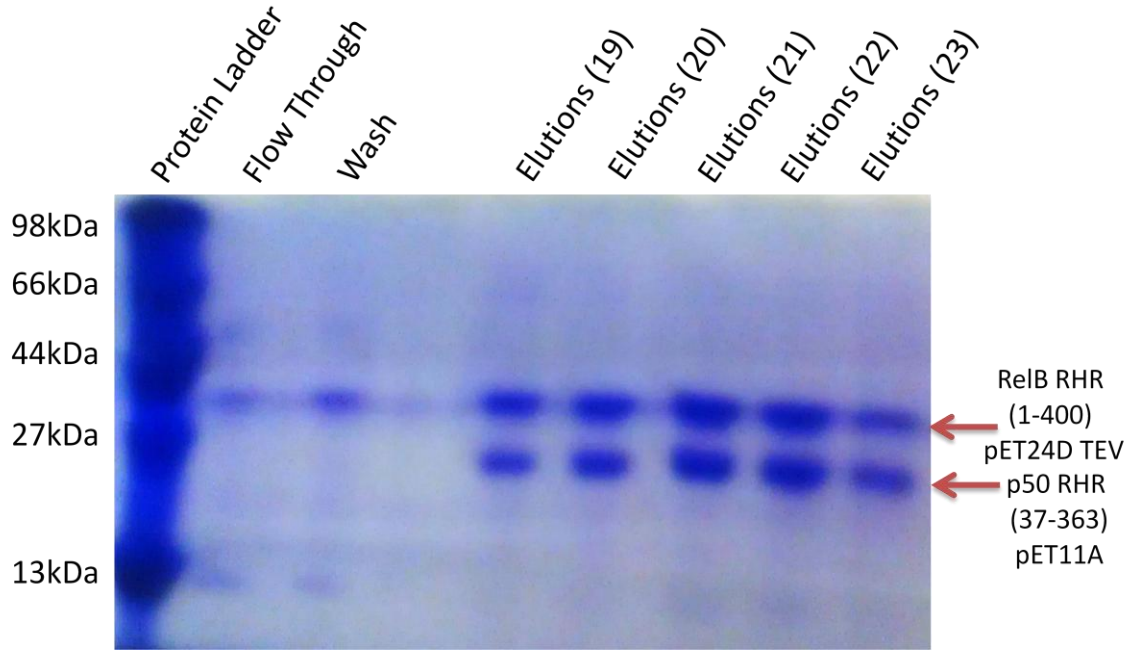

Figure 17: Purification of Murine p50 RHR (37-363) pET11A:Murine RelB RHR(1-400) pET24D TEV Heterodimer. The purified proteins were denatured, refolded, and re-purified once they formed a complex through HiTrapS column using NaCl gradient. They are now analyzed on 12.5% SDS PAGE Gel.

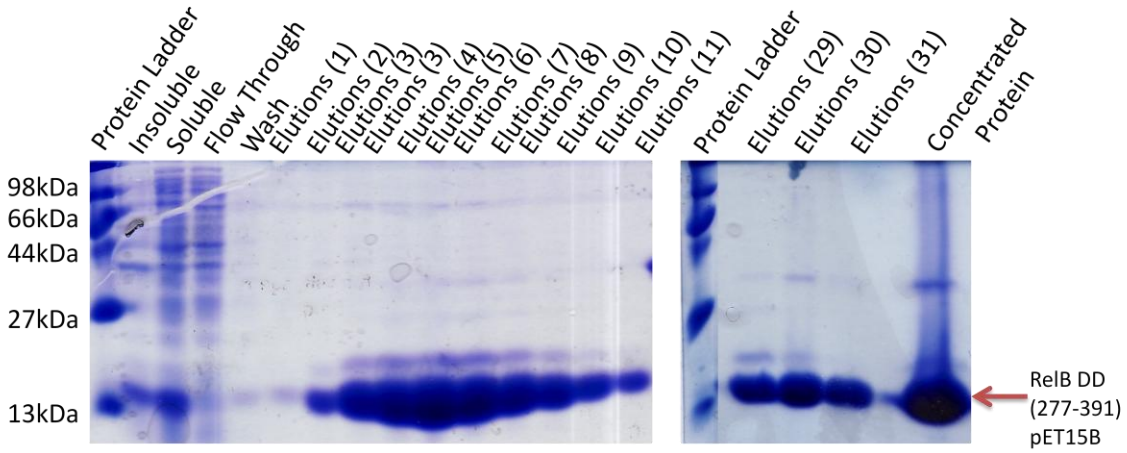

Figure 18: Purification of RelB DD (277-391) pET15B.The plasmid was expressed in BL21DE3 cell. The protein was purified via Ni^{++} column and SD75 gel filtration column, which is analyzed on 15% SDS PAGE Gel.

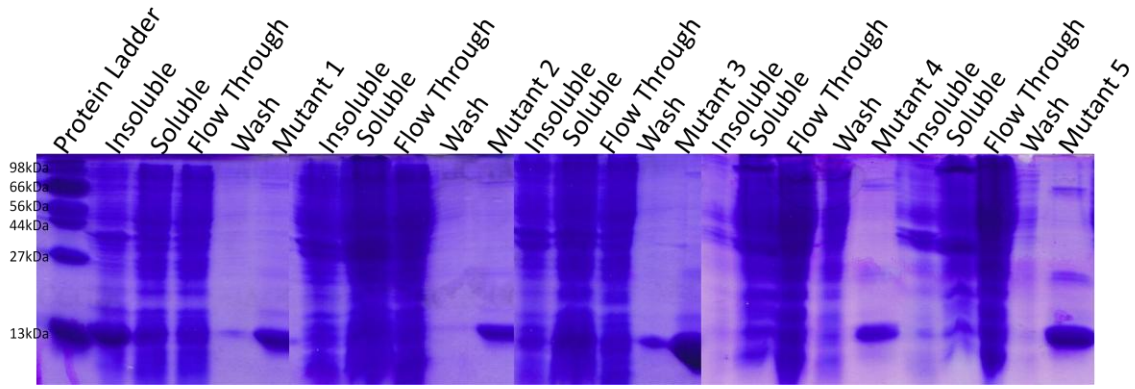

Figure 19: Purification of RelB DD (277-391) pET15B Mutants. The plasmid was expressed in BL21DE3 cell and purified using Ni_{++} which is analyzed on 15% SDS PAGE Gel. Mutant 1: RelBDD N287D, Mutant2: RelBDD Y300A, Mutant3: RelBDD I335F, Mutant4: RelBDD I286M I335F, and Mutant5: RelBDD Y300F I335F.

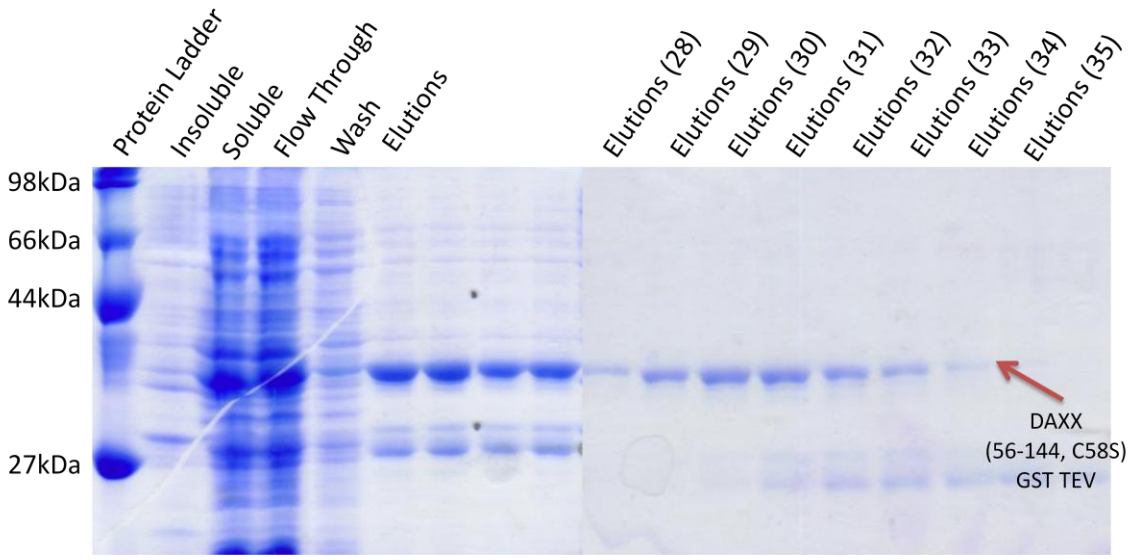

Figure 20: Protein Purification of Daxx (56-144, C58S) GST TEV. The plasmid was expressed in BL21DE3 cell, purified via GST column followed by SD200 gel filtration column, and analyzed on 10% SDS PAGE Gel.

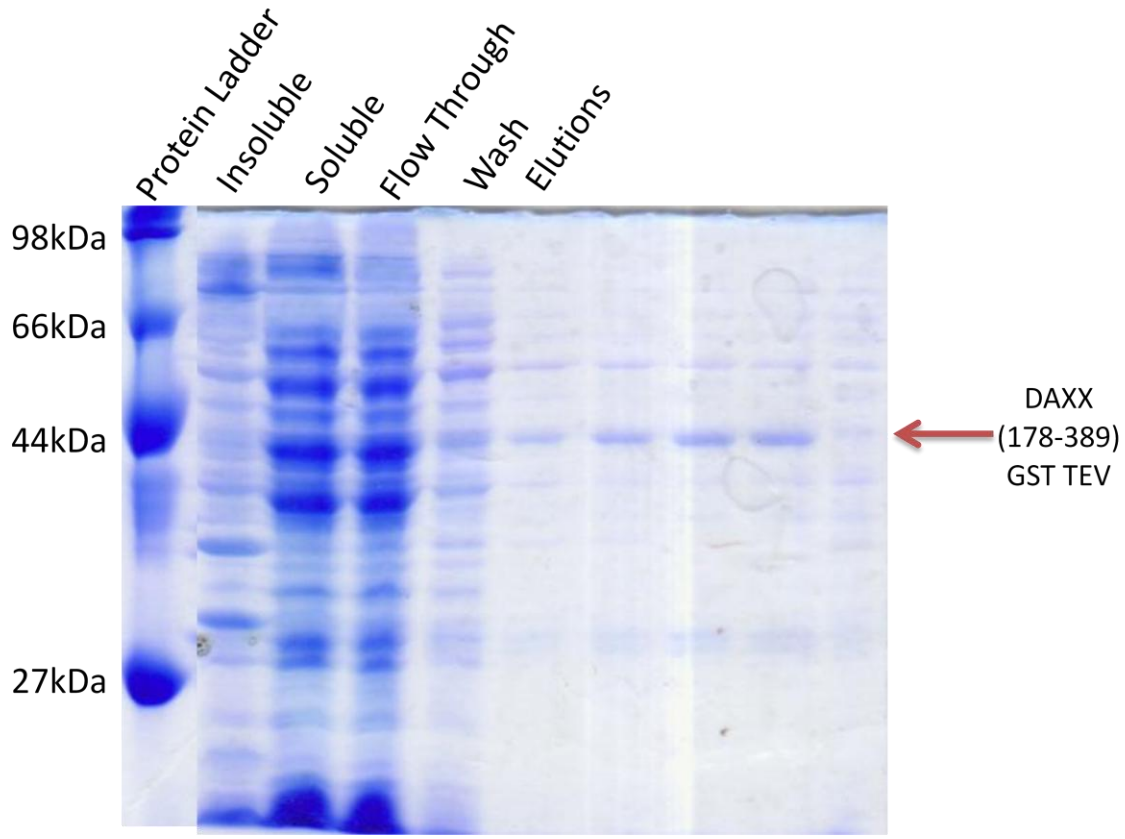

Figure 21: Protein Purification of Daxx (178-389) GST TEV. The plasmid was expressed in BL21DE3 cell, purified via GST column, and analyzed on 10% SDS PAGE Gel.

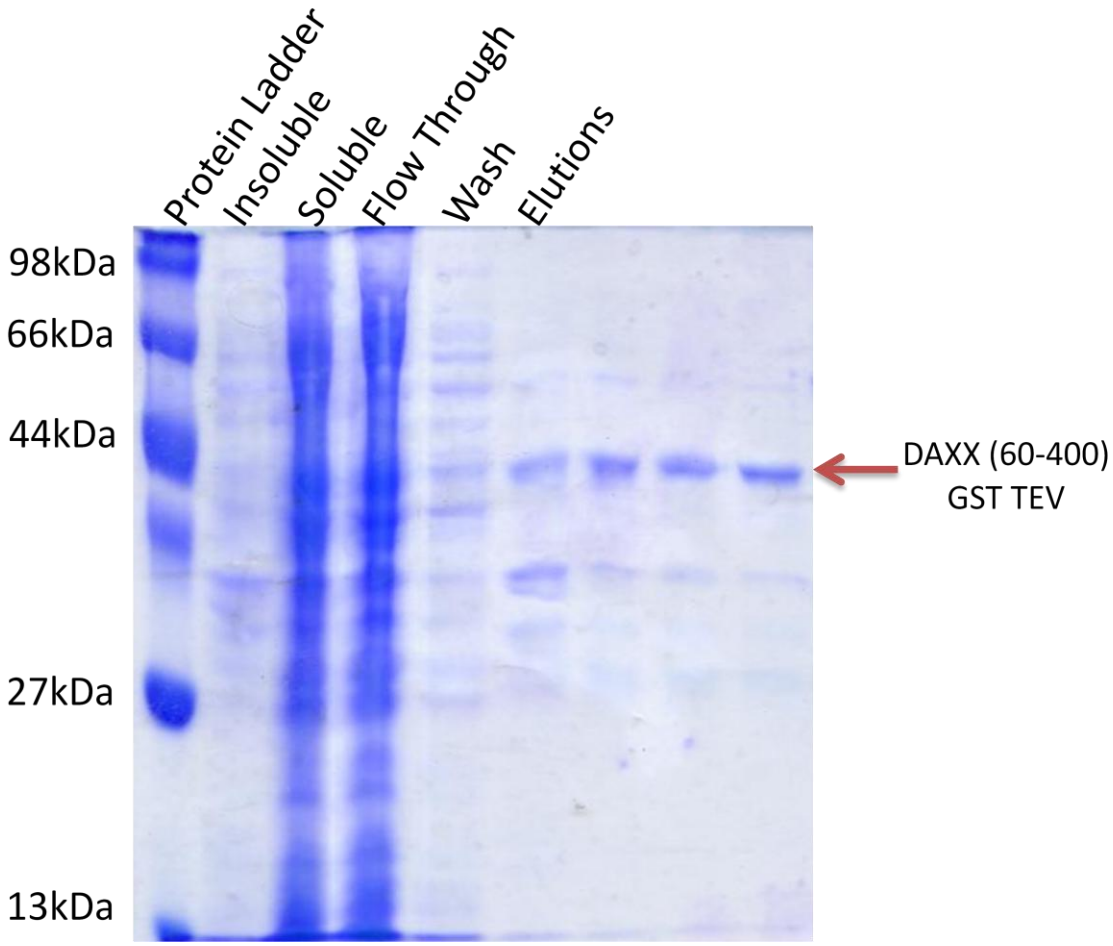

Figure 22: Purification of Daxx (60-400) GST TEV. The plasmid was expressed in BL21DE3 cell, purified via GST column, and analyzed on 10% SDS PAGE Gel.

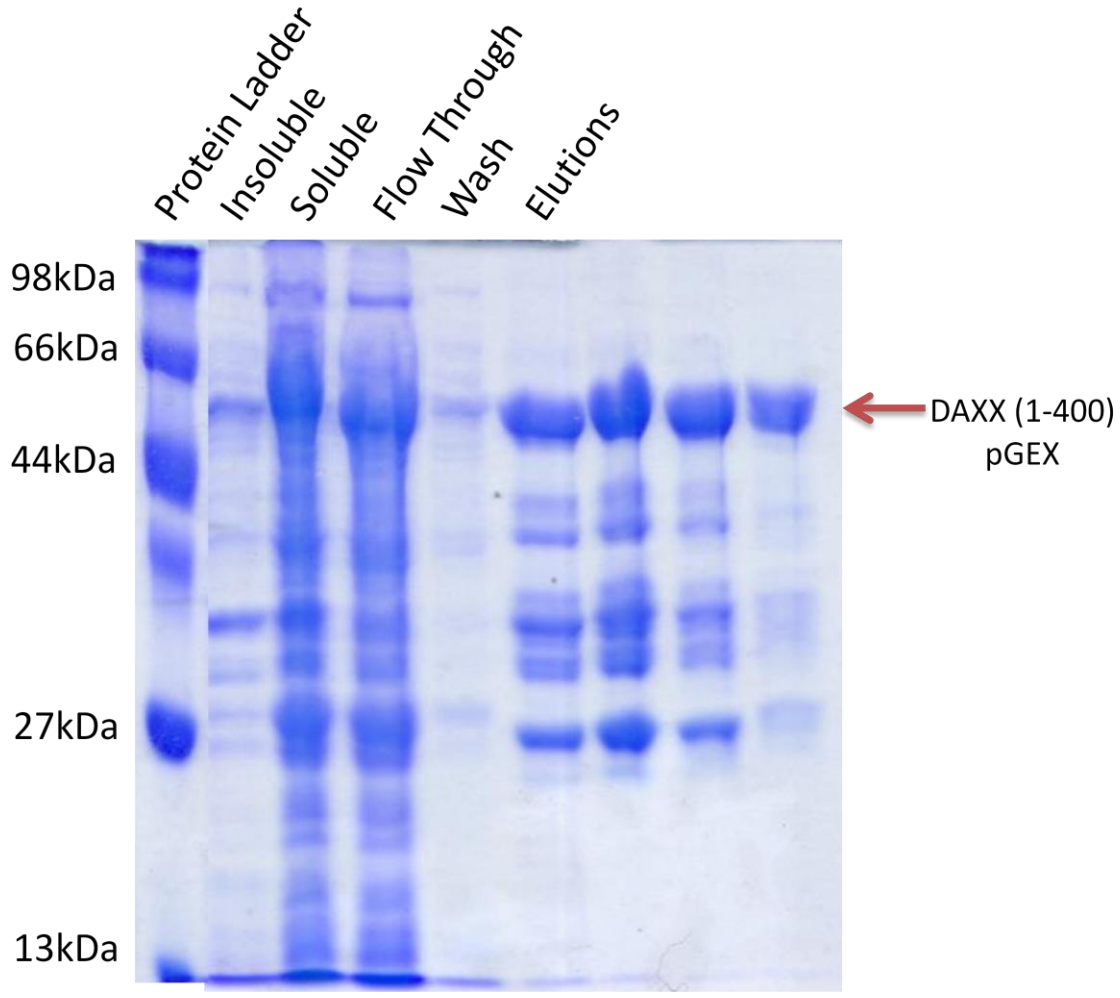

Figure 23: Purification of Daxx (1-400) pGEX. The plasmid was expressed in BL21DE3 cell, purified over GST column, and analyzed on 10% SDS PAGE Gel.

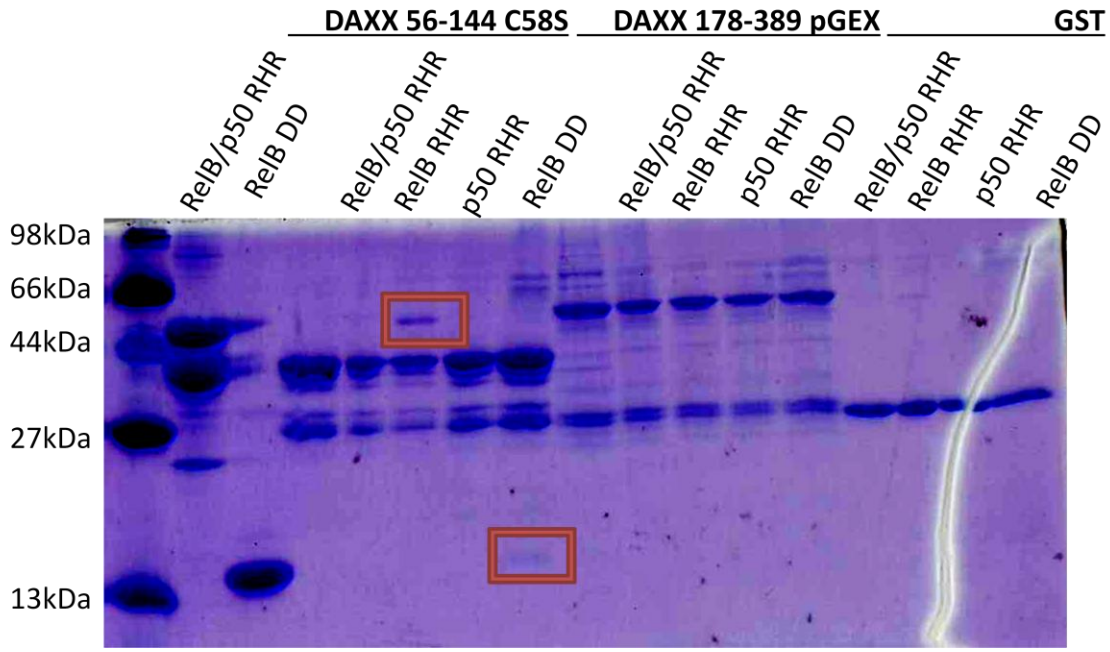

Figure 24: GST Pulldown Assay of Daxx DHBI and Daxx DHBII GST with RelB, p50, and RelB:p50 Heterodimer. The pulldown results are analyzed on 12.5% SDS PAGE Gel.

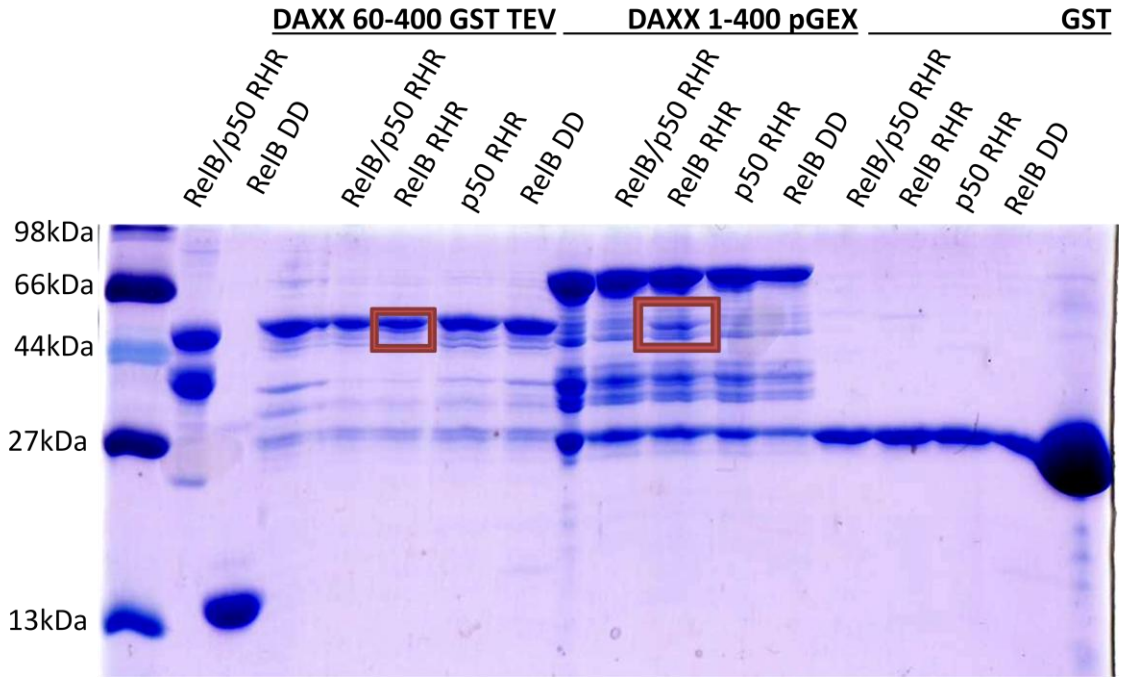

Figure 25: GST Pulldown Assay of Daxx DHBI+II and GST-tagged Daxx *N*-terminus with RelB, p50, and RelB:p50 Heterodimer. The pulldown results are analyzed on 12.5% SDS PAGE Gel.

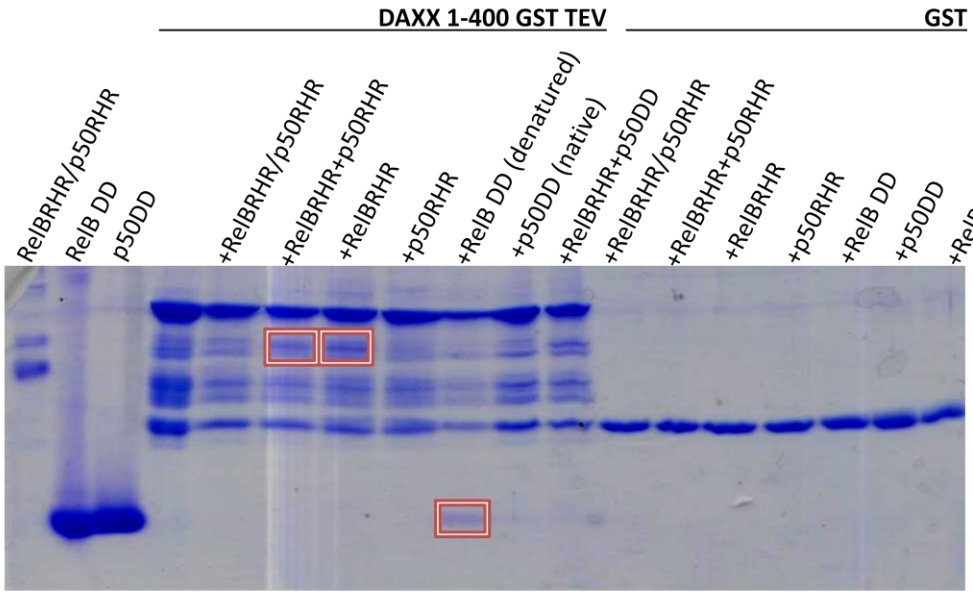

Figure 26: GST Pulldown Assay of Daxx *N*-terminus GST with RelB, p50, and RelB:p50 Heterodimer.The pulldown results are analyzed on 12.% SDS PAGE Gel.

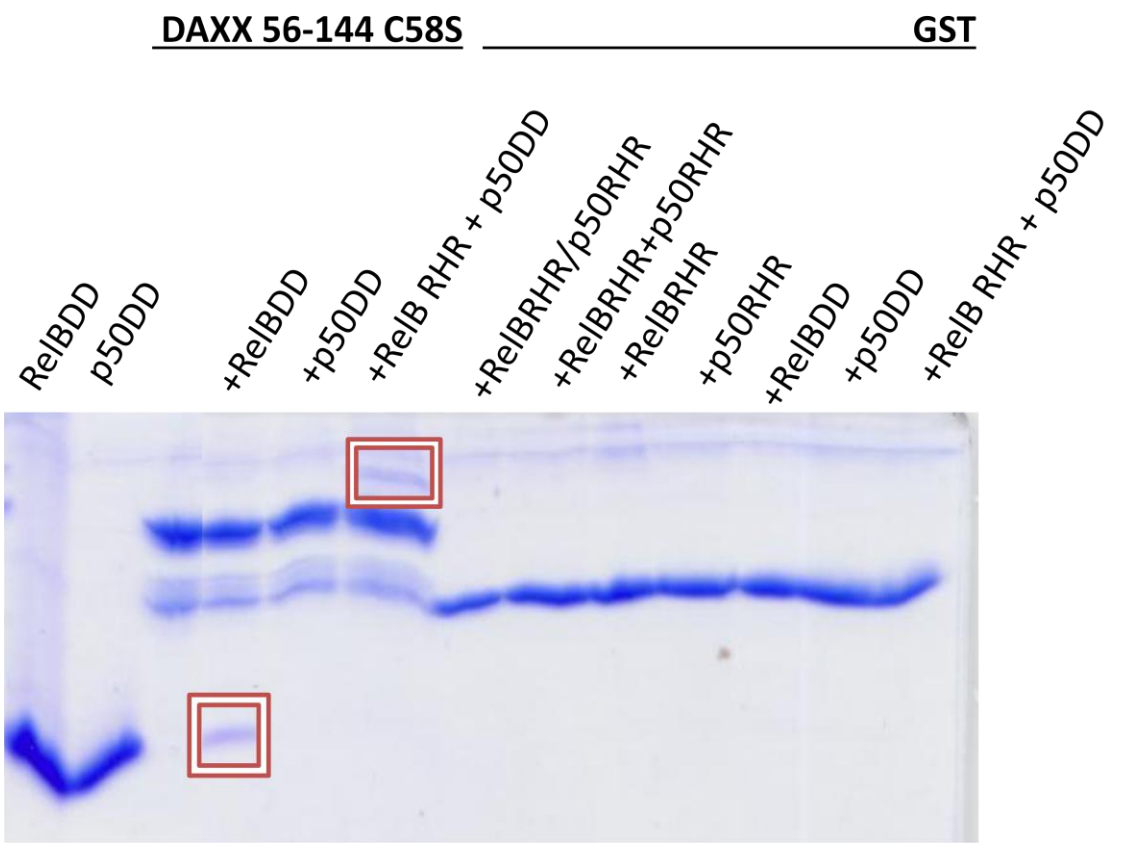

Figure 27: GST Pulldown Assay of Daxx DHBI GST with RelB, p50, and RelB:p50 Heterodimer. The pulldown results are analyzed on 12.5% SDS PAGE Gel.

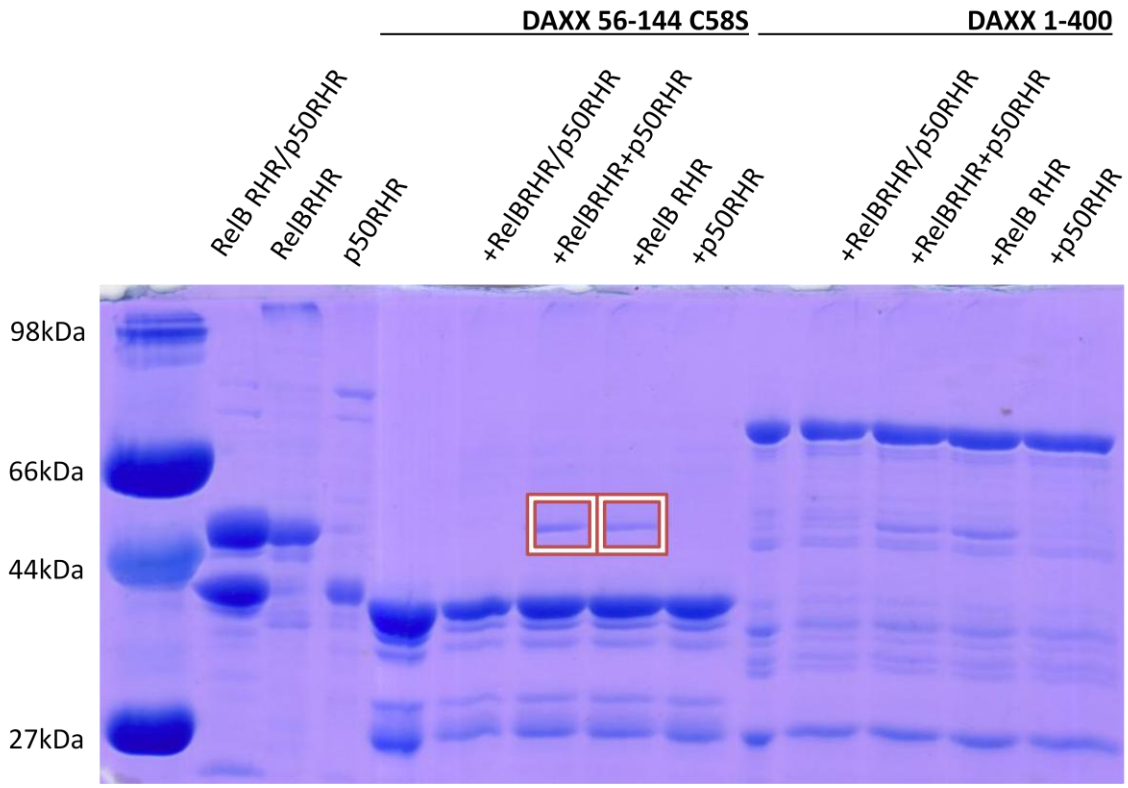

Figure 28: GST Pulldown Assay of Daxx DHBI and GST-tagged Daxx *N*-terminus with RelB, p50, and RelB:p50 Heterodimer. The pulldown results are analyzed on 10% SDS PAGE Gel.

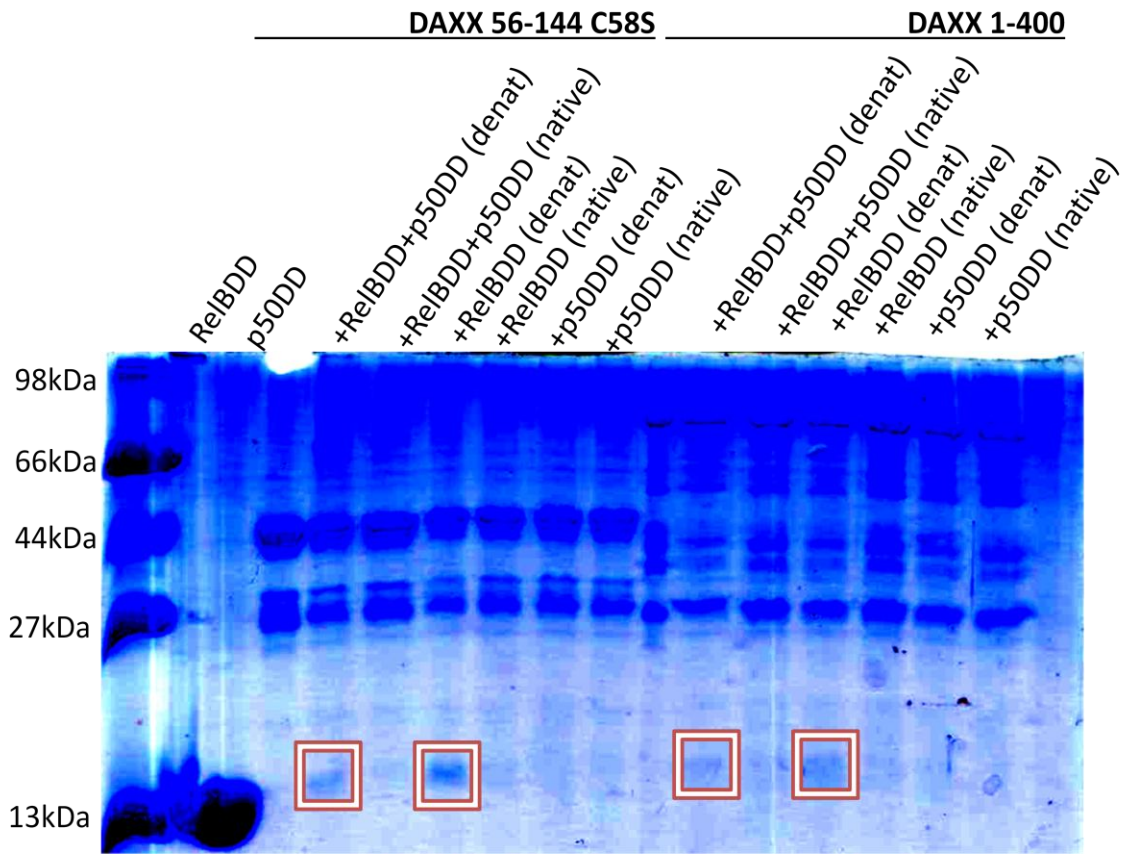

Figure 29: GST Pulldown Assay of Daxx DHBI and GST-tagged Daxx *N*-terminus with RelBDD and p50 DD. The pulldown results are analyzed on 16% SDS PAGE Gel.

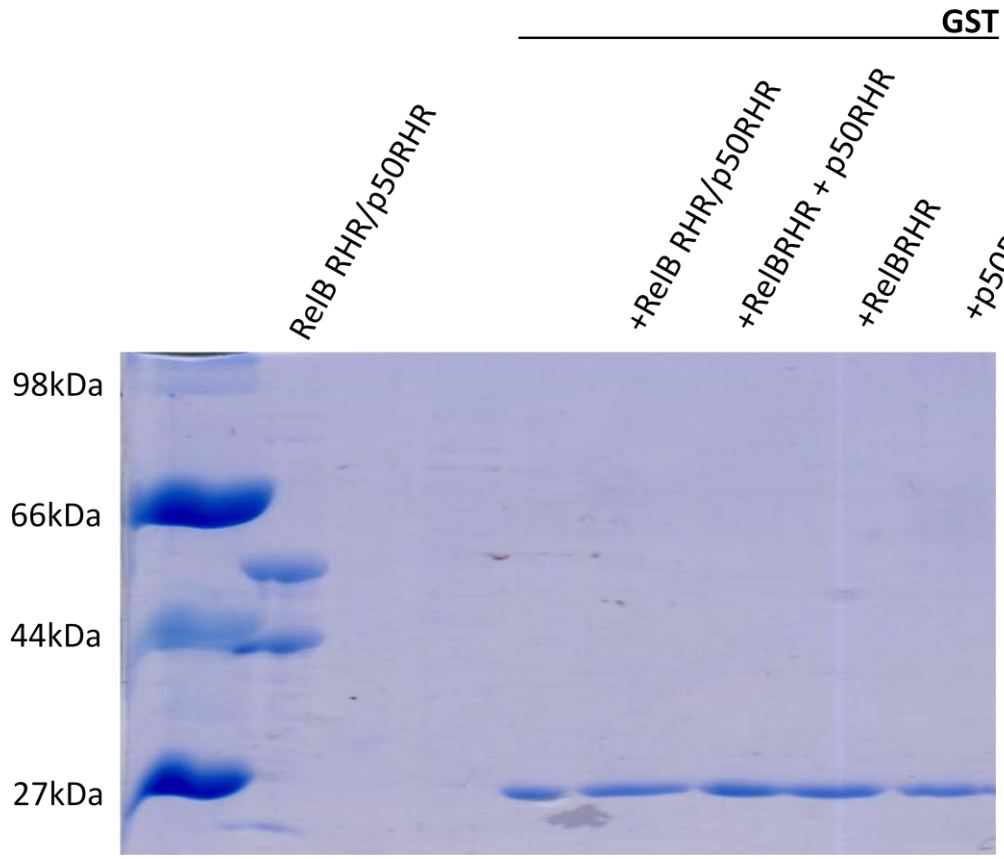

Figure 30: GST Pulldown Assay of GST Controls with RelB, p50, and RelB:p50. The pulldown results are analyzed on 12% SDS PAGE Gel.

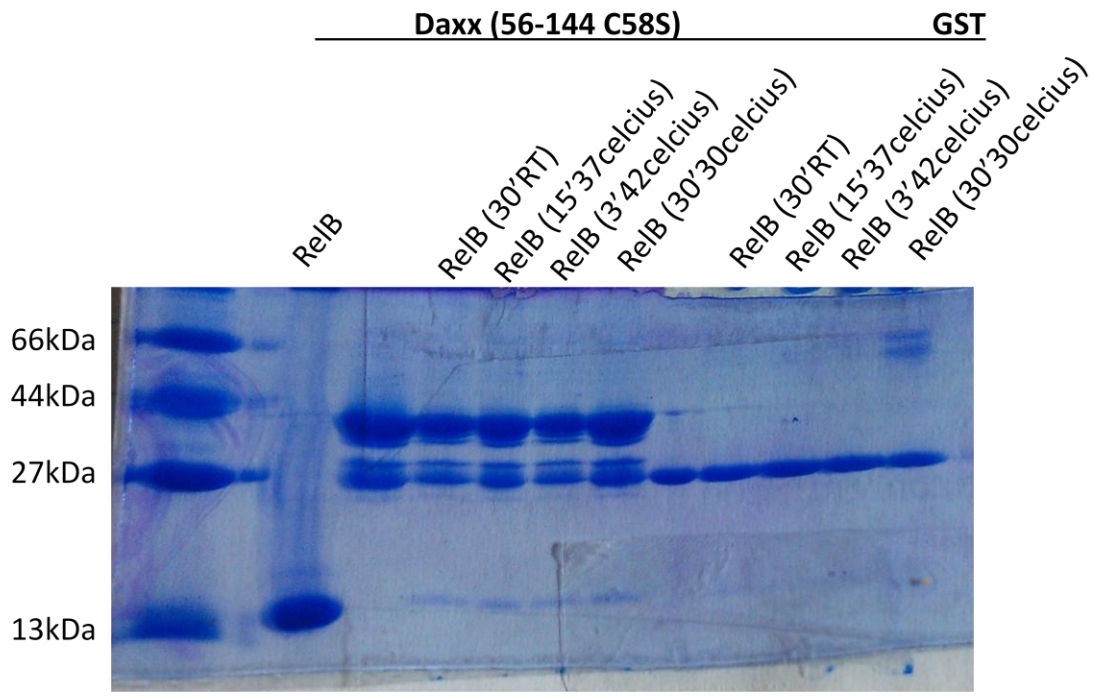

Figure 31: GST Pulldown Assay of Daxx GST with RelB DD (277-391) Based on Temperature Variation. The pulldown results are analyzed on 15% SDS PAGE Gel.

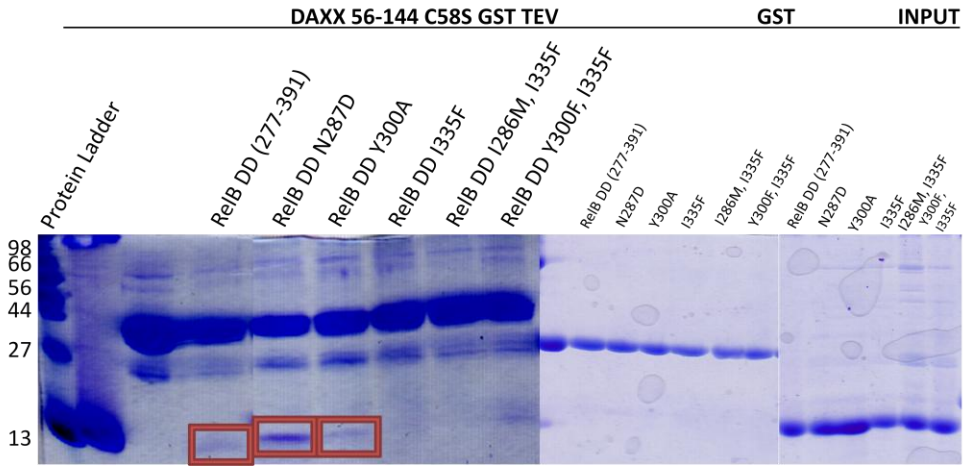

Figure 32: GST Pulldown Assay of Daxx GST with RelB DD (277-391) Mutants. The pulldown results are analyzed on 15% SDS PAGE Gel.

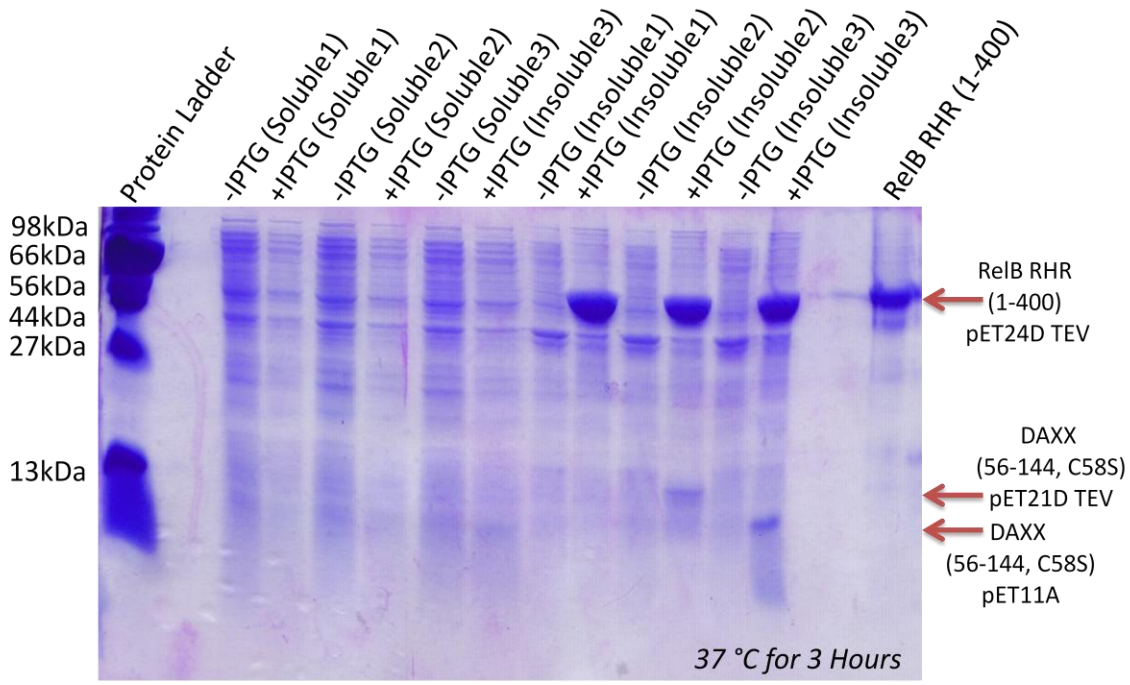

Figure 33: Expression Check for Co-Expressed RelB RHR (1-400) pET24D, Daxx (56-144, C58S) in Different DAXX Constructs. The plasmids were transformed in BL21DE3 cell and were induced at OD 0.5 with 1.0 mM IPTG. 1: RelB RHR (1-400) pET24D, axx(56-144, C58S) GST TEV, 2: RelB RHR (1-400) pET24D, Daxx (56-144, C58S) pET24D TEV, and 3: RelB RHR (1-400) pET24D, Daxx (56-144, C58S) pET 11A.

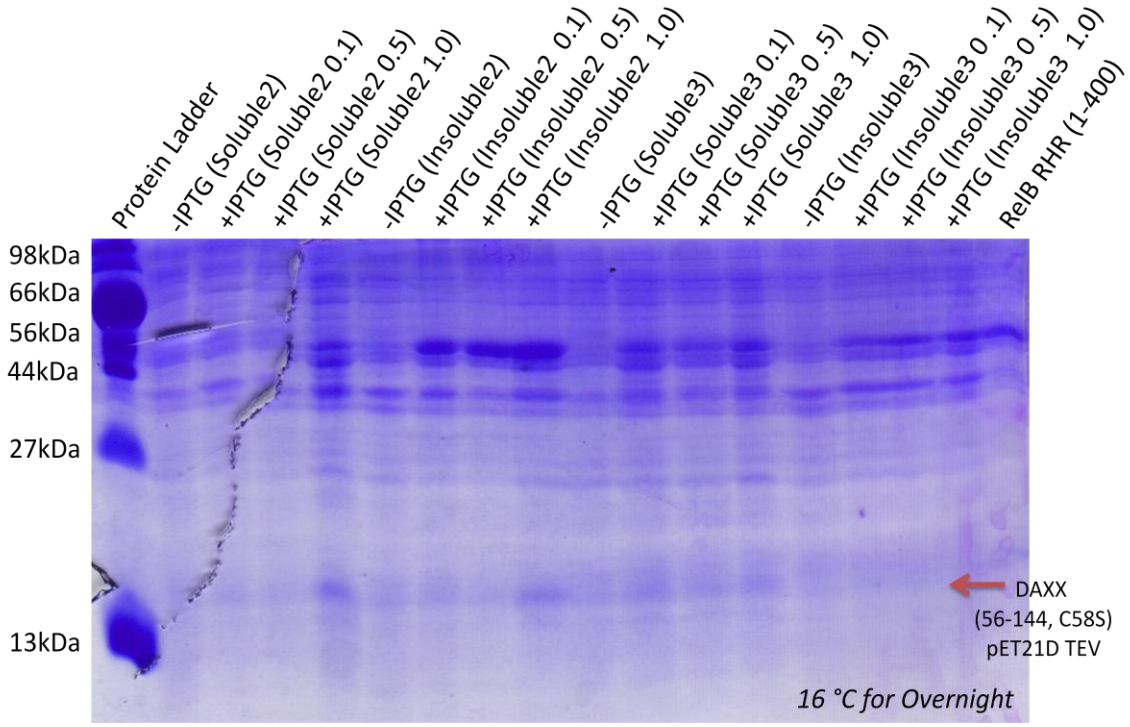

Figure 34: Expression Check for Co-Expressed RelB RHR (1-400) pET24D, Daxx (56-144, C58S) in Different Daxx Constructs. Plasmids were transformed in BL21DE3 cell, grown till OD reached 0.5, and induced with different concentrations of IPTG (0.1, 0.5, and 1.0 mM) for 16 °C overnight. 2: RelB RHR (1-400) pET24D, Daxx (56-144, C58S) pET24D TEV, 3: RelB RHR (1-400) pET24D, Daxx (56-144, C58S) pET 11A.

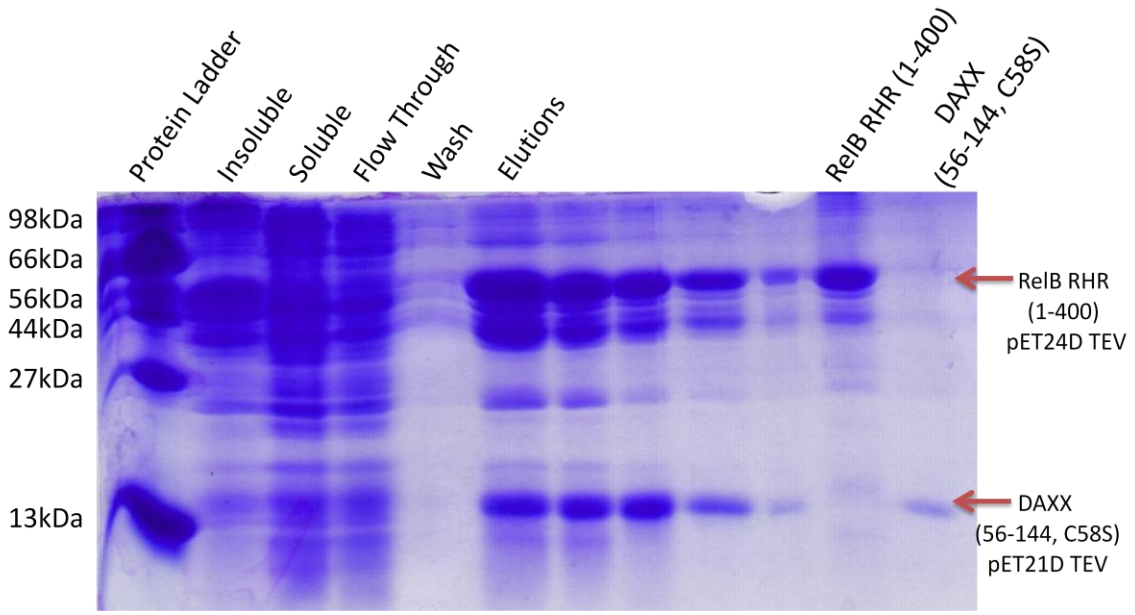

Figure 35: Protein Purification of Co-Expressed RelB RHR (1-400) pET24D:Daxx (56-144, C58S) pET24D TEV. The plasmids were transformed in BL21DE3 cell, purified via Ni^{++} column, and analyzed on 15% SDS PAGE Gel.

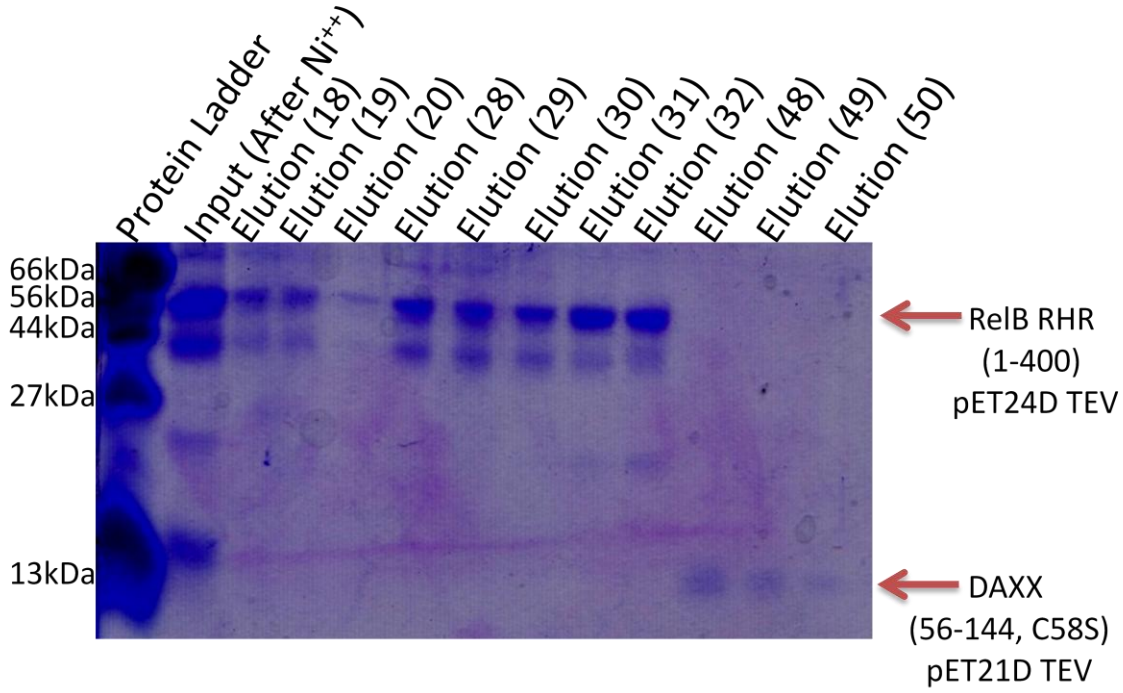

Figure 36: Protein Purification of Co-Expressed RelB RHR (1-400) pET24D:Daxx(56-144, C58S) pET24D TEV. The purified proteins from Figure 35 were further purified using SD200 gel filtration which are then analyzed on 15% SDS PAGE Gel.

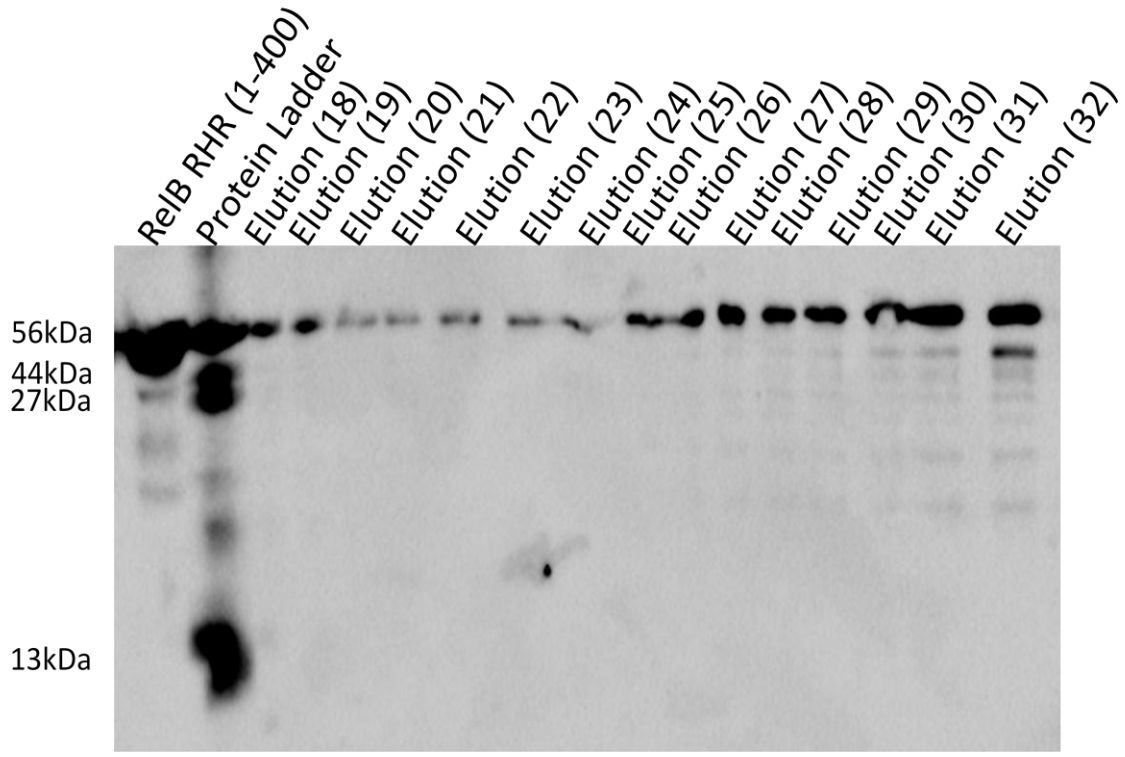

Figure 37: Protein Purification of Co-Expressed RelB RHR (1-400) pET24D:Daxx (56-144, C58S) pET24D TEV. The purified proteins from Figure 36 were further analyzed using Western Blot (αHis) since both Daxx DHBI and RelB RHR are in His-tag containing vectors. The results are analyzed on 15% SDS PAGE Gel.

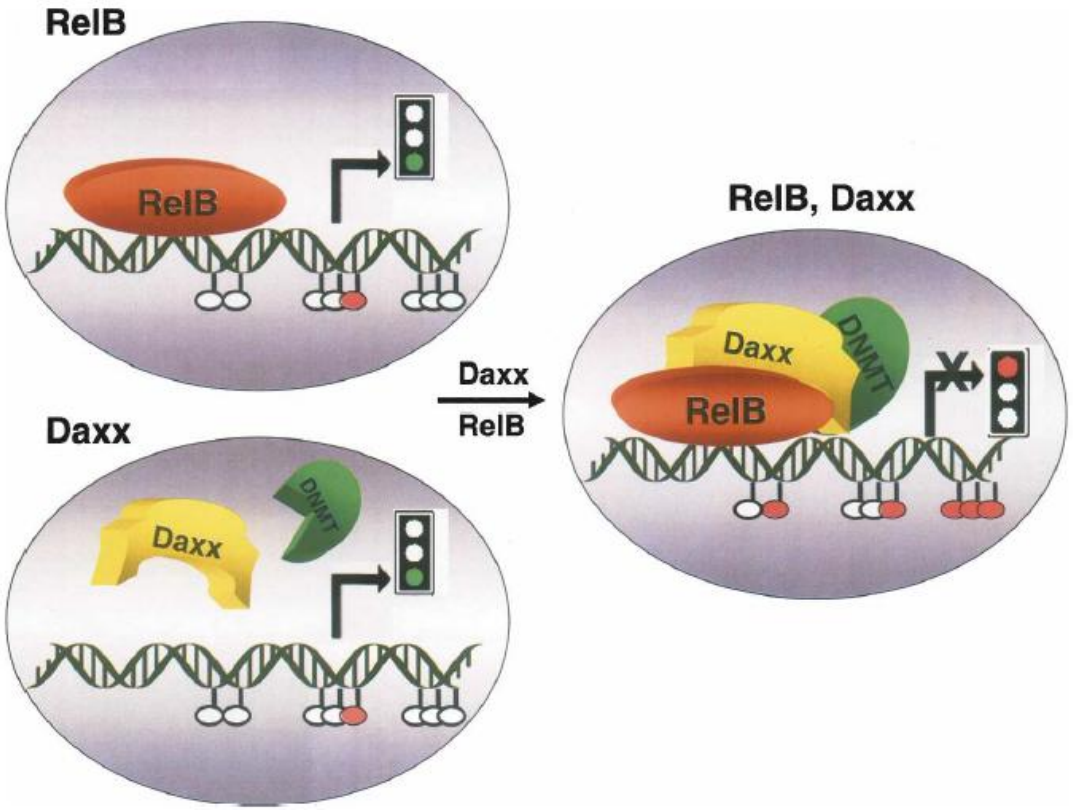

Figure 38: Daxx and RelB Interaction Diagram. Daxx binds to RelB to turn off transcription of DNA by binding to RelB which can bind to DNMT (DNA methyltransferase) (Puto *et al.*, 2007).

Table 1: List of Primers Used for RelB and Daxx Sub-Cloning in Polymerase Chain Reaction.

Name of Primer (With Cut Site Used)	Sequence (5'->3') *Cut Site in Lower Case; Sequence in Capital; Base Pair Change in Color	Vector Used
RelB (277-x)BamHI	gc gga tcc AAC ACA TCG GAG CTG CGG ATT TGC	pET 24D TEV (His)
RelB (x-391)HindIII w/ STOP	gc aag ctt tca CCG CTT TCG CTT CTT GTC CAC	pET 24D TEV (His)
Daxx (56-X, C58S) BamHI	gc gga tcc AAG AAA TcC TAC AAG CTG GAG	GST TEV based on pET 21D
Daxx (x-144) EcoRI	gc gaattc GTT CAG CTT CTT TTT GGC TGA	GST TEV based on pET 21D
Daxx (178-X) BamHI	gc ggatcc TCT CCA AGG ACC CGT GGT TCC	GST TEV based on pET 21D
Daxx (X-389) EcoRI	gc gaattc GCC CTC CTC ACT TTT GTC TTG	GST TEV based on pET 21D
Daxx (56-X, C58S) BamHI	gc gga tcc AAG AAA TcC TAC AAG CTG GAG	pET 21D TEV (His)
DAXX (x-144) HindIII w/ STOP	gc aag ctt tca GTT CAG CTT CTT TTT GGC TGA	pET 21D TEV (His)
DAXX (56-X, C58S) NdeI	gc cat atg AAG AAA TcC TAC AAG CTG GAG	pET11A (Non-Tag)
Daxx (x-144) BamHI w/ STOP	gc gga tcc tca GTT CAG CTT CTT TTT GGC TGA	pET11A (Non-Tag)

Table 2: List of Primers Used for RelB Dimerization Domain Mutagensis in Polymerase Chain Reaction.

Name of Primer	Sequence (5'->3') *Base Pair Change in Color	Vector Used
RelBDD I286M (TOP)	CTG CGG ATT TGC CGA ATG AAC AAG GAG AGC GGG	pET15B
RelBDD I286M (BOTTOM)	CCC GCT CTC CTT GTT CAT TCG GCA AAT CCG CAG	pET15B
RelBDD N287D (TOP)	CTG CGG ATT TGC CGA ATC GAC AAG GAG AGC GGG	pET15B
RelBDD N287D (BOTTOM)	CCC GCT CTC CTT GTC GAT TCG GCA AAT CCG CAG	pET15B
RelBDD Y300F (TOP)	GGT GGT GAG GAG CTG TTC TTG CTC TGT GAC AAG	pET15B
RelBDD Y300F (BOTTOM)	CTT GTC ACA GAG CAA GAA CAG CTC CTC ACC ACC	pET15B
RelBDD Y300A (TOP)	GGT GGT GAG GAG CTG GCC TTG CTC TGT GAC AAG	pET15B
RelBDD Y300A (BOTTOM)	CTT GTC ACA GAG CAA GGC CAG CTC CTC ACC ACC	pET15B
RelBDD I335F (TOP)	C GTG CAC CGG CAG TTT GCC ATT GTG TTC AAG	pET15B
RelBDD I335F (BOTTOM)	CTT GAA CAC AAT GGC AAA CTG CCG GTG CAC G	pET15B
RelBDD L371K (TOP)	GTG TGC AGC GAG CCG AAG CCC TTC ACG TAC CTG	pET15B
RelBDD L371K (BOTTOM)	CAG GTA CGT GAA GGG CTT CGG CTC GCT GCA CAC	pET15B

References

Baeuerle P, Baltimore D. 1988. I_B: a specific inhibitor of the NF-_B transcription factor. *Science* 242:540–46

Baldwin, A. S., Jr (1996). The NF-kappa B and I kappa B proteins: new discoveries and insights. Annu. Rev. Immunol. 14, 649–683

Chang CC, Naik MT, Huang YS, Jeng JC, Liao PH, Kuo HY, Ho CC, Hsieh YL, Lin CH, Huang NJ, Naik NM, Kung CC, Lin SY, Chen RH, Chang KS, Huang TH, Shih HM. Structural and functional roles of Daxx SIM phosphorylation in SUMO paralog-selective binding and apoptosis modulation. Mol Cell. 2011 Apr 8;42(1):62-74. doi: 10.1016/j.molcel.2011.02.022. PubMed PMID: 21474068.

Croxton R, Puto LA, de Belle I, Thomas M, Torii S, Hanaii F, Cuddy M, Reed JC. Daxx represses expression of a subset of antiapoptotic genes regulated by nuclear factor-kappaB. Cancer Res. 2006 Sep 15;66(18):9026-35. PubMed PMID: 16982744.

Curtin JF, Cotter TG. Live and let die: regulatory mechanisms in Fas-mediated apoptosis. Cell Signal. 2003 Nov;15(11):983-92. Review. PubMed PMID: 14499341.

De-Bin Huang, Don Vu, Gourisankar Ghosh, NF-κB RelB Forms an Intertwined Homodimer, Structure, Volume 13, Issue 9, September 2005, Pages 1365-1373, ISSN 0969-2126, 10.1016/j.str.2005.06.018.

Dobrzanski, P., Ryseck, R. P. & Bravo, R. (1993). Both N-and C-terminal domains of RelB are required for full transactivation: role of the N-terminal leucine zipper-like motif. Mol. Cell. Biol. 13, 1572–1582.

Escobar-Cabrera E, Lau DK, Giovinazzi S, Ishov AM, McIntosh LP. Structural characterization of the DAXX N-terminal helical bundle domain and its complex with Rassf1C. Structure. 2010 Dec 8;18(12):1642-53. doi: 10.1016/j.str.2010.09.016. PubMed PMID: 21134643.

Escobar-Cabrera E, Okon M, Lau DK, Dart CF, Bonvin AM, McIntosh LP. Characterizing the N- and C-terminal Small ubiquitin-like modifier (SUMO)-interacting motifs of the scaffold protein DAXX. J Biol Chem. 2011 Jun 3;286(22):19816-29. doi: 10.1074/jbc.M111.231647. Epub 2011 Mar 7. PubMed PMID: 21383010; PubMed Central PMCID: PMC3103359.

Hayden MS, Ghosh S. Shared principles in NF-kappaB signaling. *Cell* 2008; **132**:344-362.

Liu CP, Xiong C, Wang M, Yu Z, Yang N, Chen P, Zhang Z, Li G, Xu RM. Structure of the variant histone H3.3-H4 heterodimer in complex with its chaperone DAXX.Nat

Struct Mol Biol. 2012 Dec;19(12):1287-92. doi: 10.1038/nsmb.2439. Epub 2012 Nov 11. PubMed PMID: 23142979.

Li R, Pei H, Watson DK, Papas TS. EAP1/Daxx interacts with ETS1 and represses transcriptional activation of ETS1 target genes. Oncogene. 2000 Feb 10;19(6):745-53. PubMed PMID: 10698492.

Moorthy AK, Huang DB, Wang VY, Vu D, Ghosh G. X-ray structure of a NF-kappaB p50/RelB/DNA complex reveals assembly of multiple dimers on tandem kappaB sites. J Mol Biol. 2007 Oct 26;373(3):723-34. Epub 2007 Aug 22. PubMed PMID: 17869269.

Puto LA, Reed JC. Daxx represses RelB target promoters via DNA methyltransferase recruitment and DNA hypermethylation. Genes Dev. 2008 Apr 15;22(8):998-1010. doi: 10.1101/gad.1632208. PubMed PMID: 18413714; PubMed Central PMCID: PMC2335332.

Ruben, S. M., Klement, J. F., Coleman, T. A., Maher, M., Chen, C. H. & Rosen, C. A. (1992). I-Rel: a novel rel-related protein that inhibits NF-kappa B transcriptional activity. Genes Dev. 6, 745–760.

Ryseck, R. P., Bull, P., Takamiya, M., Bours, V., Siebenlist, U., Dobrzanski, P. & Bravo, R. (1992). RelB, a new Rel family transcription activator that can interact with p50-NF-kappa B. Mol. Cell. Biol. 12, 674–684.

Salomoni P, Khelifi AF. Daxx: death or survival protein? Trends Cell Biol. 2006 Feb;16(2):97-104. Epub 2006 Jan 10. Review. PubMed PMID: 16406523.

Sen R, Baltimore D. 1986. Inducibility of_ immunoglobulin enhancer-binding protein NF-_B by a post-translational mechanism. *Cell* 47:921–28

Sen R, Baltimore D. 1986. Multiple nuclear factors interact with the immunoglobulin enhancer sequences. *Cell* 46:705–16

Sun SC, Ley SC. New insights into NF-kappaB regulation and function. *Trends Immunol* 2008; **29**:469-478.

Vallabhapurapu S, Karin M. Regulation and function of NFkappaB transcription factors in the immune system. *Annu Rev Immunol* 2009; **27**:693-733.

Yang X, Khosravi-Far R, Chang HY, Baltimore D. Daxx, a novel Fas-binding protein that activates JNK and apoptosis. Cell. 1997 Jun 27;89(7):1067-76. PubMed PMID: 9215629; PubMed Central PMCID: PMC2989411.

Zhang H, He J, Li J, Tian D, Gu L, Zhou M. Methylation of RASSF1A gene promoter is regulated by p53 and DAXX. FASEB J. 2013 Jan;27(1):232-42. doi: 10.1096/fj.12-215491. Epub 2012 Oct 4. PubMed PMID: 23038753; PubMed Central PMCID: PMC3528318.